Jb. Geol. B.-A.	ISSN 0016-7800	Band 131	Heft 1	S. 169–201	Wien, Juni 1988

Rb-Sr Isotopic Resetting in Mylonites and Pseudotachylites: Implications for the Detachment and Thrusting of the Austroalpine Basement Nappes in the Eastern Alps

By MARTIN THÖNI*)

With 22 Figures and 5 Tables

Tirol
Mylonite
Pseudotachylite
Rb-Sr thin slab dating
Isotopic resetting
Alpine shear zones
Austroalpine basement units
Eo-Alpine event
Detachment and thrusting
Ötztal-Stubai complex
Silvretta basement

Österreichische Karte 1 : 50.000
Blätter 143–148, 169–175

Contents

Zusammenfassung

Die polymetamorphen ostalpinen Grundgebirgsdecken der Tiroler Zentralalpen und Ost-Graubündens zeigen stark unterschiedliche kretazisch-metamorphe Überprägung. Im Ötztal-Stubai-Kristallin etwa steigert sich diese alpidische Metamorphose nordwest-südostwärts von anchizonalen bis zu amphibolitfaziellen Bedingungen.

Der jüngste, regional verbreitete Strukturtyp in diesen Gesteinen ist eine offene Stauchfaltung (chevron-type) mit meist steiler Achsialflächenorientierung. Auf Grund mikrostruktureller und geochronologischer Daten ist für manche dieser mit D_3 signierten Strukturen spätvariszisches Alter wahrscheinlich; dies gilt zumindest für jene Bereiche, wo die alpidischen Überprägungstemperaturen niedrig blieben.

In diesen alpidisch schwach geheizten Abschnitten des Grundgebirges werden ältere Lithologien und Strukturen lokal von meist flach liegenden Scherzonen unterschiedlicher Dimension (cm-m-Bereich) diskordant zerschnitten. Der Deformationsstil in diesen Zonen ist semiduktil bis duktil, in Verbindung mit unterschiedlicher und meist intensiver Retrogradierung des voralpidischen Mineralbestandes. Makro- und mikroskopische Schersinnindikatoren weisen häufig auf ost–west- bis südost–nordwest-, in Einzelfällen auch auf nordvergente Scherbewegungen in diesen Zonen hin. Im regionalen Rahmen können diese jungen Deformationszonen als kleinräumige Analoga der Schliniglinie aufgefaßt werden; entlang dieser Bewegungszone ist intra-ostalpine Zerscherung des Grundgebirges im Ausmaß von mindestens 40 km belegt.

Im Zuge lokaler Kataklase, bevorzugter Kanalisierung und Interaktion von Fluids mit dem Gestein sowie fortschreitender Deformation und dynamischer Rekristallisation wurde das Rb-Sr-Isotopensystem im Kleinbereich unterschiedlich stark beeinflußt. Modell- und Regressionsalter, die aufgrund mikrostruktureller Kriterien als geologisch signifikant interpretiert

*) Author's address: Univ.-Doz. Dr. MARTIN THÖNI, Institut für Geologie, Universität Wien, Universitätsstraße 7/III, A-1010 Wien.

werden, fallen in den Zeitraum 90–70 Mio. J. Damit überlappen diese Deformationsalter zeitlich weitgehend mit jenen Werten, die die regionale kretazische (Re-)Kristallisation und Abkühlung datieren. Zwei Rb-Sr-Kleinbereichsisochronenalter an Pseudotachyliten aus den Basalanteilen der Silvretta fallen mit 78.5 ±4.6 und 73 ±3.2 Mio. J. in dasselbe Zeitintervall.

In Übereinstimmung mit Petrologie-, Struktur- und Isotopendaten an nicht mylonitisierten Paragenesen des weiteren Untersuchungsgebietes können die vorliegenden Ergebnisse die Vorstellung großräumiger Abscherungs- und intrakrustaler Zerscherungsvorgänge für die Oberkreide unterstützen. Großtektonisch können diese Prozesse mit der ersten, in der frühen Oberkreide vermuteten Kontinent-Kontinent-Kollision der Adria- und der Briançonia-Platte in Verbindung gebracht werden.

Abstract

Within the polymetamorphic Austroalpine basement nappes of the Tyrolian Alps and easternmost Switzerland, eo-Alpine metamorphic overprinting increases continuously northwest-southeastwards from lowest greenschist to the staurolite-kyanite grade.

The youngest penetrative structures to be observed in these rocks is a chevron-type folding or kinking. Whereas the age of this deformation is unclear for the Alpine higher grade, extensively recrystallized parts of the profile, microstructural and small-scale Rb-Sr data support a Late Hercynian formation of similar structures in those areas that suffered only weak Alpine reheating.

Within these Alpine cooler parts of the basement, in places a non-penetrative shear-deformation is superimposed locally on older structures and lithologies, causing intense retrogression of the pre-Alpine parageneses. These semiductile to ductile, mostly flat lying shear zones range in scale from cm to m and may be traced over some hundreds of meters within otherwise homogeneous basement rocks. Macro- and microscopic shear sense indicators point frequently to a top E (SE) over W (NW) movement direction. The Schlinig thrust, along which intra-Austroalpine displacement is proven over some 40 km, shows similar characteristics and is seen as a large-scale counterpart of the smaller intra-basement shear zones.

Microfracturing, subsequent preferred fluid channelling, fluid-rock interaction and selective dynamic recrystallization caused variable resetting of the Rb-Sr isotopic system on the small scale. Model and regression ages from mylonitic parageneses, interpreted on microstructural grounds as being geologically meaningful range between 90 und 70 Ma, thus overlapping with the ages obtained for eo-Alpine regional (re-)crystallization and cooling. Two pseudotachylite samples from the basal parts of the Silvretta basement gave thin slab isochron age results of 78.5 ±4.6 and 73 ±3.2 Ma (2σ), respectively.

In connection with petrological, structural and isotopic results from non-mylonitic parageneses, the new data are interpreted as providing evidence for large-scale crustal detachment and intra-crustal fracturing, extension and thrusting processes, following a phase of compression related to continental collision of the Adriatic and Briançonian microplates in the early Late Cretaceous.

1. Introduction

The exact timing of distinct deformation events in metamorphic rocks by isotopic methods has proven to be generally more difficult than the reconstruction of thermal histories. This may partly be due to the fact that regional temperature rise and fall is more uniform for a given area, whereas intensity, rate and timing of deformation may vary considerably, even on the small scale. On the other hand, however, it is almost the rule rather than the exception, that analytically well-defined "ages" of geological events based only on a few data points tend to lapse into disarray or scatter as large amounts of data are accumulated, and different cases and rock types are studied. In regional metamorphic terrains, and especially when dealing with polymetamorphic rocks, such growing scatter with increasing information may merely reflect the natural variability of different parameters used for the final reconstruction of PTt paths. In other words the interaction of heating, deformation, recrystallization and thermal relaxation my be rather complex and heterochronous on a smaller scale (CHAMBERLAIN & KARABINOS, 1987), but may reflect continuity and contemporaneity on a wider scale and within larger time brackets. In any case, structure elements exhibiting very similar phenomenological characteristics may be considerably different in age; this applies particularly for low-grade polymetamorphic terrains, and if no clear overprinting relationships are observed, even the relative timing of distinct deformation events may fail.

For the present purpose, lithologically homogeneous metamorphic tectonites are grouped into two classes:

a) rocks with penetrative deformation textures and
b) rocks that show local non-penetrative deformation features related to late-metamorphic non-coaxial shearing or faulting.

Whereas penetrative rock deformation implies mostly conditions of elevated temperatures, where the threshold values for plastic deformation mechanisms being active in the principal constituent minerals are surpassed (e. g. VOLL, 1980; SIMPSON, 1985), shearing and faulting is of a more discrete nature (SEGALL & SIMPSON, 1986; SINHA et al., 1986) and may be active at a low to very low metamorphic grade. Initiation and nature of rock deformation are, on the other hand, strongly dependent on whether or not water is present; as a consequence, hydrolytic weakening and local deformation softening seriously enhance isotopic homogenization processes and chemical mobility in general (KIRBY, 1980; YARDLEY, 1981; WALTHER & ORVILLE, 1982; ETHERIDGE et al., 1983). Penetrative deformation of water-rich sediments undergoing metamorphism is preferentially active in the prograde temperature branch (NORRIS & HENLEY, 1976; FYFE, 1976); because of these connexions, microstructural relationships are often thermally overprinted during late-tectonic uplift and relaxation.

During these processes radioactive parent/daughter systems may be influenced by two basically different processes: diffusion and recrystallization. Whereas recrystallization is strongly dependent on intensity and rate of strain, first-order kinetic processes like volume diffusion are known to react most sensitive to temperature (DODSON, 1973, 1976), and become successively significant at higher temperatures. In higher grade regional metamorphic terrains (ca. ≥500°C) these inherent properties of solids pose strict limitations for the geochronologist. Most geochronological systems record only some stage of the cooling path (possibly with the exception of U-Pb dating of zircon, not shown in Fig. 1), and even this may be difficult to trace if cooling is very slow. Using conventional radiometric methods, like K-Ar and Rb-Sr, it is generally not possible to date early-metamorphic deformation events or even a metamorphic climax, in amphibolite or higher grade rocks with sufficient reliability.

As indicated in Fig. 1, mineral samples are generally more readily susceptible to open-system behaviour

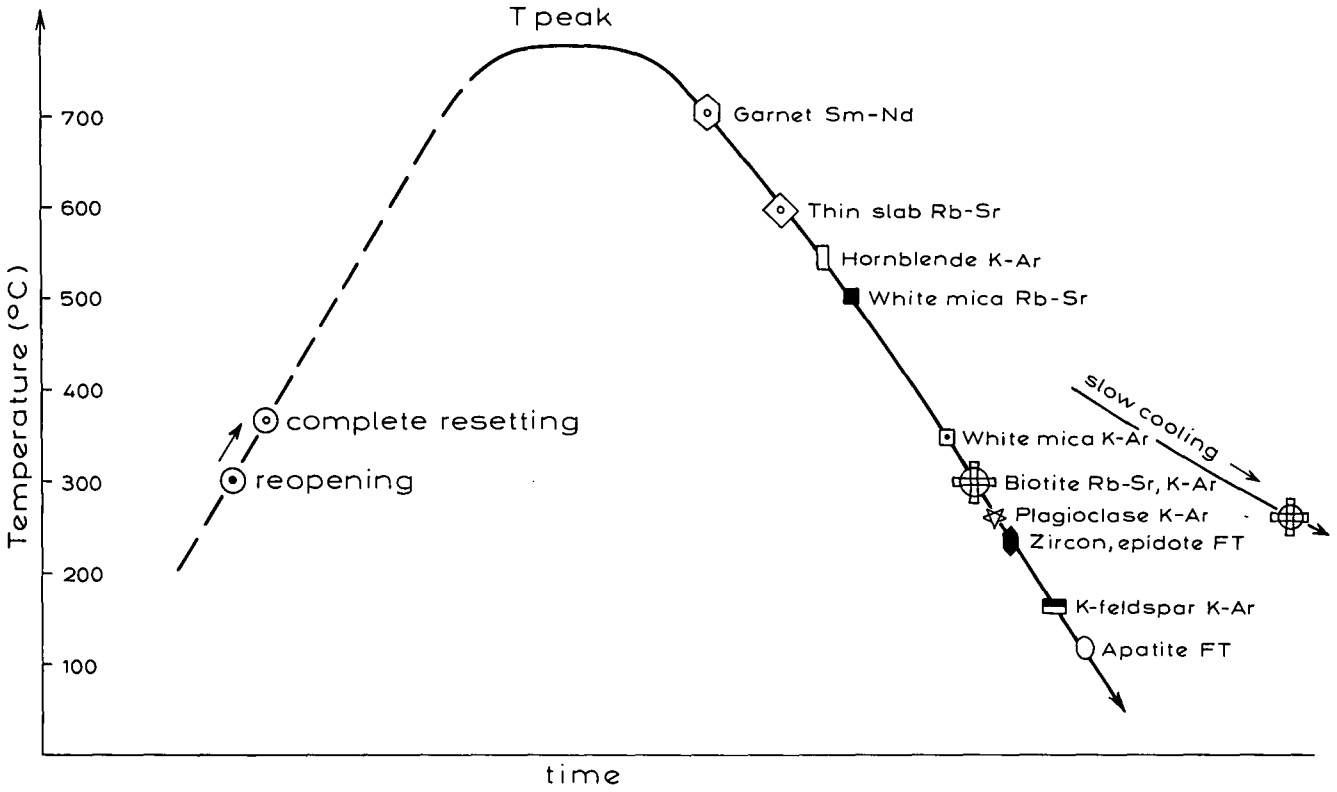

Fig. 1.
Diagrammatic representation of some published closure temperatures (T_c) in cooling geochronological systems, along a hypothetical cooling curve.
Values shown may be applied for intermediate cooling rates ($\dot{T}$ in the range of 10^7 years) and grain sizes typical for crystalline rocks (ca. 0.1–1 mm).
On the left, the branch of rising temperatures is shown schematically by the broken line; the arrow indicates that for the case of reheating a "dry" basement, and at sufficiently rapid temperature rise, temperatures necessary for complete resetting probably have to be somewhat higher than those where first reopening ($\approx T_c$) is suggested to take place (or, correspondingly, to a long time of heating, if maximum T remains constant close to T_c). Very slow cooling, on the other hand, shifts T_c to lower values, because more time for re-equilibration is available (DODSON, 1973; see indication on the right). The effective closure temperature is thus, among other things, a function of the cooling rate $\dot{T}$.
Data from HUMPHRIES & CLIFF (1982); GRIFFIN & BRUECKNER (1985); AFTALION & VAN BREEMEN (1980); HARRISON (1981); PURDY & JÄGER (1976), HARRISON et al. (1979); HURFORD (1986), WAGNER et al. (1977).

and thus to metamorphic resetting than whole-rock systems. This applies, of course, only to largely dewatered (higher grade) metamorphic rocks, where temperature is a ubiquitously dominant influencing factor and migration distances of istopes are primarily related to thermal diffusion rates rather than to the mobilization and transport by a fluid phase. Despite the very large amount of informations concerning the temperature dependence of isotopic systems, as gained from laboratory studies (e. g. HOFMANN, 1979; FREER, 1981), from deep bore-holes (DEL MORO et al., 1982) and especially from many different contact and regional metamorphic situations (HART, 1964; PURDY & JÄGER, 1976), the scale of isotopic (re-)equilibration during thermal pulses is still a fundamental matter of debate. This applies even to the small scale (e. g. BUHL & GRAUERT, 1985), let alone for regional or global scale dimensions (see e. g. discussion by HOFMANN & HART, 1978). Among other things, such disagreements may result from the strongly variable and complicated interaction of deformation and the fluid phase during thermal overprint and in different mineralogies.

The concept of closure temperatures in geochronological systems (PURDY & JÄGER, 1976) has recently become a matter of debate (e. g. CHOPIN & MALUSKI, 1980; VERSCHURE et al., 1980; DESMONS et al., 1982; DEUTSCH & STEIGER, 1985; ZEITLER & WIJBRANS, 1986), but is, nonetheless, still widely applied (see CLIFF, 1985 for review). Thus while it appears that temperature is one important factor, it is not the only and occasionally not even the dominant one that influences isotopic systems. Furthermore, the assumption that closing of isotopic systems during cooling and opening during reheating occur at one and the same temperature is an implicit one and probably not correct. For instance, from regional studies it was deduced that complete resetting of minerals in a reheated basement is acheived only at somewhat higher metamorphic conditions than those correspondig to closure temperatures during cooling (THÖNI, 1981). This may result from the fact that during the reheating and structural overprinting of "dry" basement rocks, pressure-solution dominated deformation mechanisms are severely reduced, unless water is introduced from the outside. Grain boundary sliding, crystal plasticity and recrystallization processes may hence also be retarded at low grade conditions. Under such circumstances, geochronological systems seem to expand their stability towards higher temperatures. Most arguments put forward against closing temperatures originate from structural observations. It is obvious, that a too strict application of a „blocking" temperature model would make it almost impossible to date low- to very low grade deformation events in polymetamorphic rocks.

The main problems encountered in dating non-penetrative structures that formed at low temperatures concern, among others

1) incomplete isotopic reworking, because of the ineffectiveness of diffusion at low temperatures and if recrystallization was incomplete, and
2) heterogeneous fluid flow combined with large strain gradients (and incomplete recrystallization) resulting in a possibly heterogeneous isotopic mobilization and/or selective isotopic leaching. As resetting or partial resetting of isotopic systems in low-temperature mylonites s. l. cannot be described by using the closing/opening temperature model, geochronologial interpretation of data gained from such rocks relies essentially on the structural interpretation, especially, if detailed microchemical investigations are not available. If such interpretations suggest complete strain-induced recrystallization, then the isotopic ages should also be geochronologically meaningful.

One further basic complication has to be mentioned at this point. Considering Rb-Sr isochrons and partly also ^{40}Ar-^{39}Ar plateau ages, it was pointed out repeatedly that utmost care is needed in giving a definitive geological significance even to well-defined, linearily arrayed data sets: isochrons may be rotated partly, preserving a primary collinear data array (e. g. VAN SCHMUS & BICKFORD, 1976; THÖNI, 1986), and extraneous ^{40}Ar may be masked in a plateaus age if distribution throughout the sample is uniform (ASHKINADSE et al., 1977; FOLAND, 1983; HUNZIKER et al., 1986). In most such cases the calculated ages are too old, but inappropriate sample combination may as well lead to (meaningless) apparent ages that are younger than the overprinting event (HICKMAN & GASSLEY, 1984). In such cases, where reliably defined geochronological data are questioned, because, for example, they conflict with geological evidence, probably only one possibility remains to find out their true significance: reproducibility of the ages on the outcrop scale, if possible using different lithologies, grain sizes or even different parent/daughter pairs. If concordance of data is exhibited within, as well as between samples, the geologic meaning of the ages should be clear; however, if this is not the case, a polyphase (heterochronous) deformation history and/or incompletely reset systems have to be reckoned with as equivalent alternatives.

Some of the problems just discussed are dealt with below. The main aim of this paper is to evaluate the geochronologic potential of the Rb-Sr thin slab and mineral dating technique for the reconstruction of distinct deformation events during structural and metamorphic overprinting, turning special attention to the combination of structural and isotopic aspects in "fault-related rocks" (WISE et al., 1984).

Sample preparation and analytical techniques

Thin whole rock slices were separated by sawing along microlayering (as defined by compositional or/and tectonic layering), then chipped and ground using standard procedures. Fine fractions were extracted by sedimentation in distilled water, after short grinding. Coarse minerals were purified by grinding in alcohol, sieving and standard magnetic separation.

Rb and Sr concentrations were determined by isotope dilution on 100–200 mg of sample, using a highly concentrated ^{87}Rb-^{84}Sr spike. Measurements were performed using a MICROMASS M30 mass spectrometer. Repeated measurements for the NBS 987 $SrCO_3$ standard during the course of this work gave a $^{87}Sr/^{86}Sr$ value of 0.71005 ±8 ($2\sigma_m$).

Isochron calculation is based on YORK (1969). In distinguishing between isochron and errorchron according to the Table of the F Variate (at the 95 per cent confidence level), the following cutoff levels are applied (see ref. in THÖNI, 1986): 5-point regression: MSWD ≤2.99, 10-point regression: MSWD ≤2.34. Following this discrimination, the regression ages as shown in Figs. 18b, 19d and 21d represent isochrons, whereas those in Figs. 17b, 20b and 21c are errorchrons.

All constants used are those recommended by STEIGER & JÄGER (1977).

Abbreviations used in the tables: B = biotite, WR = whole rock. For analytical data of samples T1521 and T1631 see THÖNI (1986).

2. Regional Geologic Outline of the Western Austroalpine Basement Units

Austroalpine basement units cover by far the greater part of the central Eastern Alps. Though in the Western Alps, this tectonically highest nappe system ist only very rudimentarily preserved, recent studies have revealed some remarkable similarities for the eo-Alpine history in the western and eastern parts of the Austroalpine domain (e.g. DAL PIAZ et al., 1972; HUNZIKER, 1974; VOGLER, 1984; OBERHÄNSLI et al., 1985; STÖCKHERT et al., 1986; MORAUF, 1980; FRANK, 1987; MILLER et al., 1987).

Plate tectonic models consider the Austroalpine nappe system to be the result of Mid-Upper Cretaceous continental collision of the Briançonian and Adriatic microplates following the subduction of the south Penninic trough (FRISCH, 1981; LAUBSCHER, 1983). Whereas earlier orogenetic models treat the Alpine edifice mainly by a S over N imbrication (e.g. CLAR, 1973; TOLLMANN, 1978), more recent structural interpretations point to a dominant (S)E over (N)W rock flow during the early evolution stages of the Austroalpine nappes (RATSCHBACHER, 1986; VOGLER, 1984).

On a regional scale, Alpine metamorphic overprint in this pre-Alpine basement increases southwards, i.e., towards the more interior parts of the mountain chain; but far in the south, along the Periadriatic lineament, very low-grade Alpine conditions are again found. Amphibolite grade metamorphism was reached over fairly large areas in the southeast (Kor- und Saualpe) and to a minor extent in the west (Ötztal).

The central-western Austroalpine domain, as considered in the present paper, between the Tauern window and eastern Switzerland, comprises different subunits, like the Ötztal-Stubai, Silvretta, Scarl and Ortler-Campo complexes (Fig. 2). Although an exact pre-orogenic position for these subunits relative to each other is not well established, they are thought to still maintain a rather primary connection. A major zone of movement is, however, documented by the Schlinig thrust, along which intra-Austroalpine displacements in the range of 30–40 km are proven (SCHMID & HAAS, 1987).

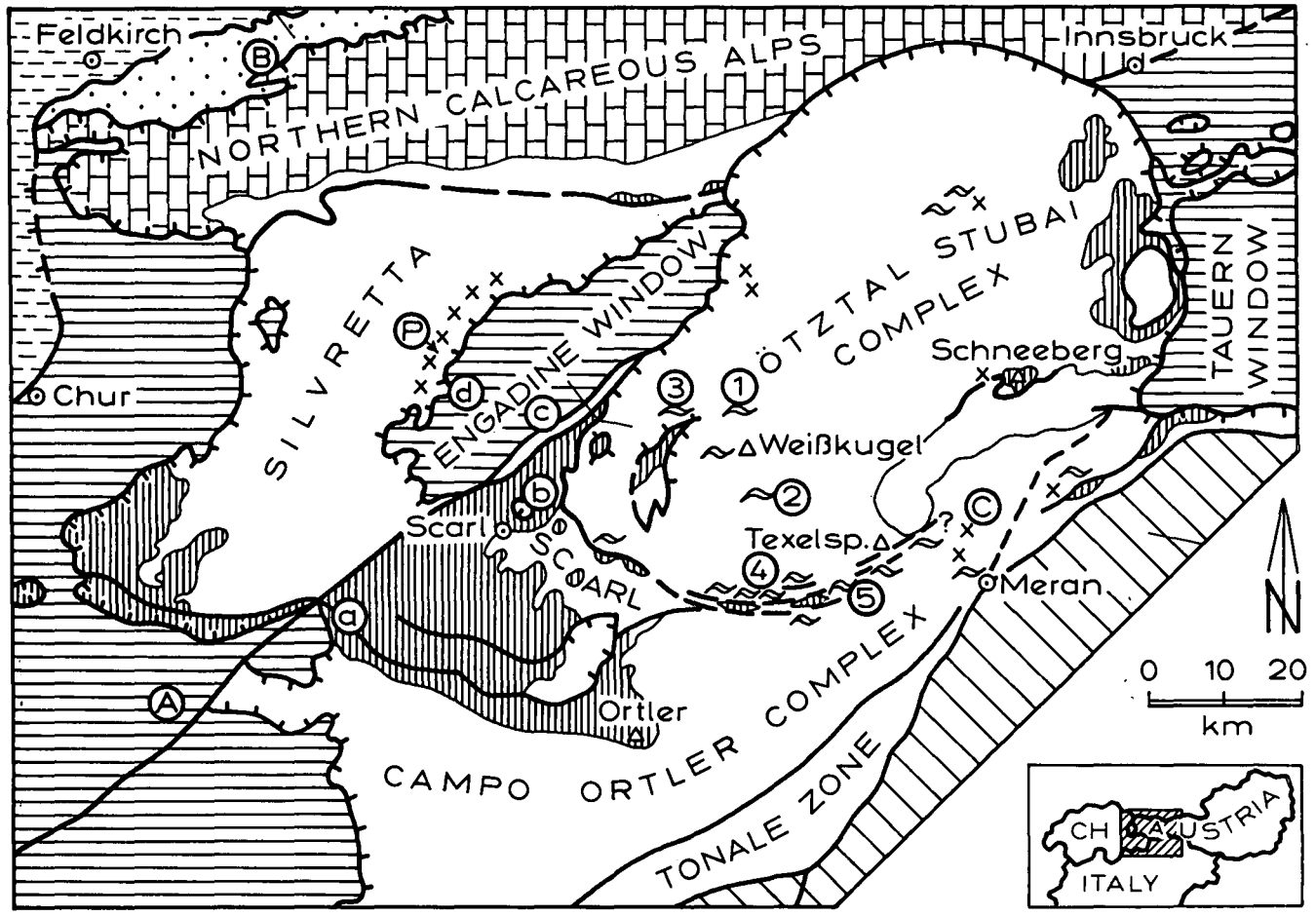

Mylonites ①-⑤, × Pseudotachylites Ⓟ, ⓐ-ⓓ Important fossil localities, Ⓐ-Ⓒ High-p minerals or assemblages

Helveticum

Flysch zone

Pennine-Lower Austroalpine (undifferentiated)

Northern Calcareous Alps

(Para-) Autochthonous Permo-mesoz. Cover / Basement, incl. Paleozoic series

Southalpine units

Austroalpine

▲ a ▼ b

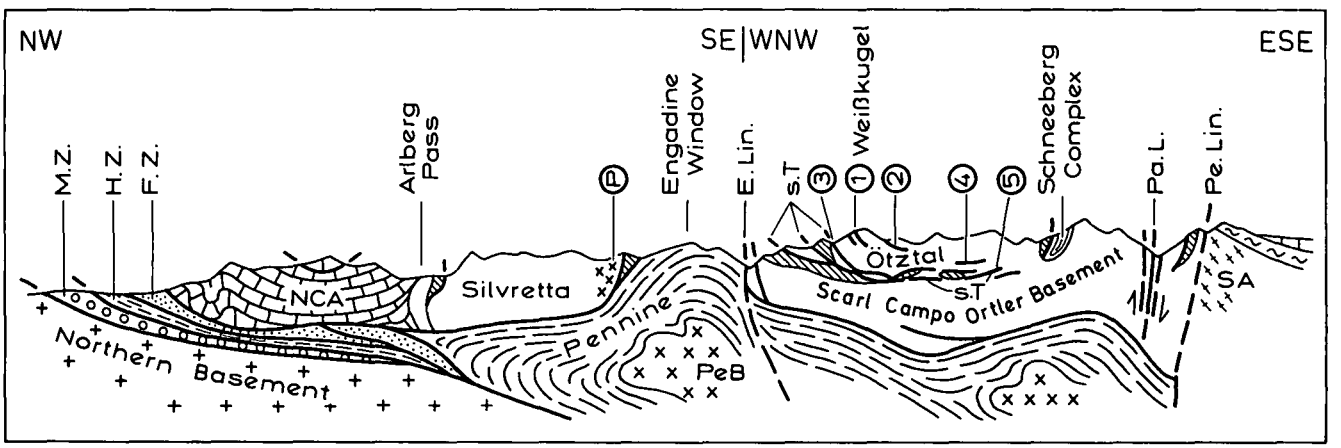

Fig. 2.

a) Sketch of the western Austroalpine basement nappes, between the Tauern window and eastern Switzerland, showing their clear allochthonous position: detachment of these units is related to the eo-Alpine (Cretaceous) continental collison, but large scale thrusting and the final emplacement lasted into Late Tertiary times.
Numbers and symbols refer to important sample localities discussed in the text and to the following references, respectively: A, DEUTSCH (1983); B, WINKLER & BERNOULLI (1986); C, HOINKES & THÖNI (1987); a, CARON et al. (1982); b, MADER (1983); c, TORRICELLI (1956); d, RUDOLPH (1982) and OBERHAUSER (1983). Obliquely ruled field (inset, lower right) marks area of investigation.

b) Schematic section across the area of investigation showing the approximate position of different tectonic units. Mean profile trend is marked by a broken line in Fig. 2a.
M.Z. = Molasse zone; H.Z. = Helveticum; F.Z. = Flysch zone; NCA = Northern Calcareous Alps; PeB = Pennine basement; E.Lin. = Engadine line; S.T. = Schlinig thrust zone; Pa.L. = Passeier line; Pe.Lin. = Periadriatic lineament; SA = Southalpine units; 1-5 and P = sample localities.

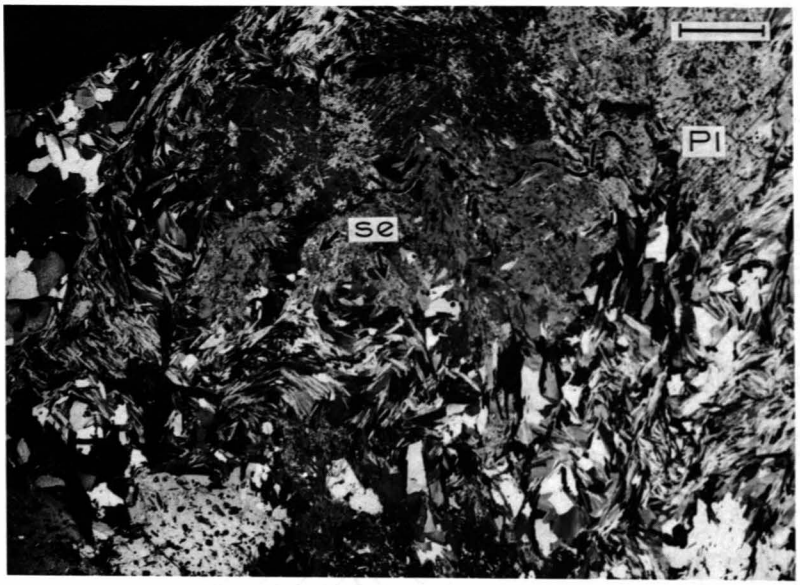

◀ a

▼ b

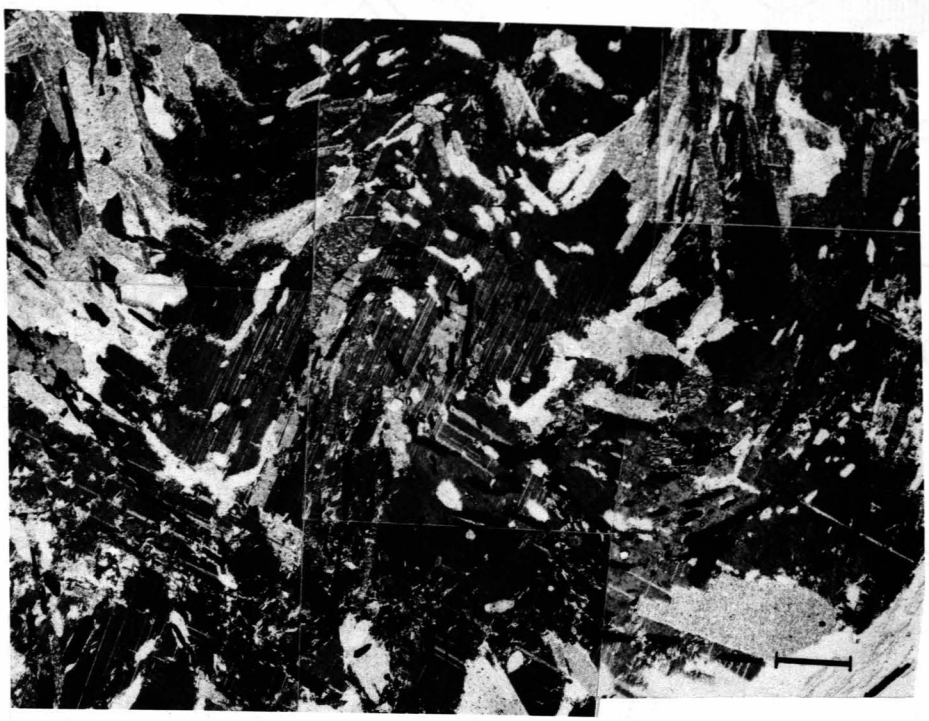

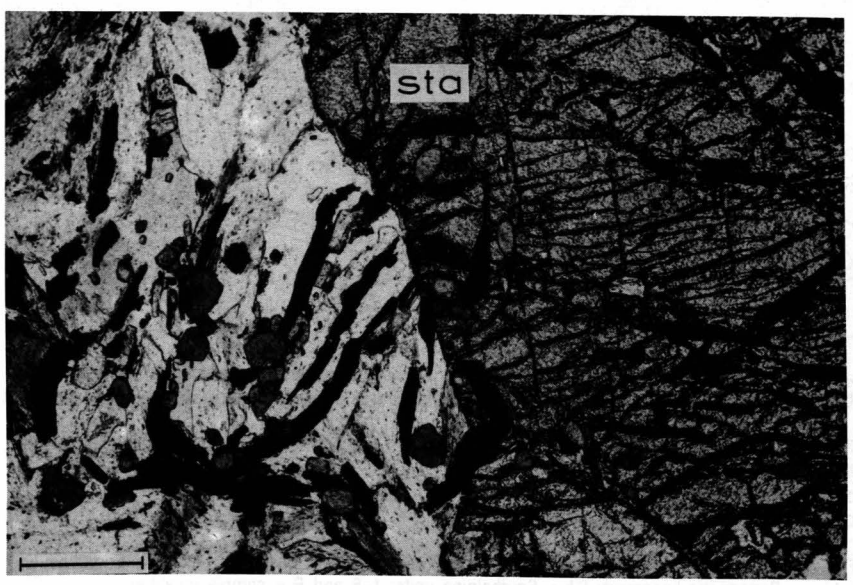

◀ c

Fig. 3.

a) Photomicrograph of a crenulated paragneiss (sample T601) from the Hercynian basement of Weißkugel area showing large plagioclase prorphyroblasts that grew over an older microfabric (e.g. inclusion trails of tourmaline, garnet and opaques within the plagioclase). Mica (lower) and quartz (left upper part) are mostly strain-free, documenting that the Hercynian metamorphic peak generally outlasted penetrative D_2 deformation. As a result of weak (probably eo-Alpine) overprinting, plagioclase shows slight "sericitization" (centre).
Scale bar = 2 mm.

b) Detail of a D_2 microfold, traced by ilmenite (black) and muscovite; the structure was postkinematically overgrown by polysynthetically twinned and zoned plagioclase.
Paragneiss sample T632, upper Pitztal.
Scale bar = 0.25 mm.

c) Detail of postkinematic staurolite that grew over a microfold outlined by ilmenite.
Sample no. as in Fig. 3b.
Scale bar = 0.25 mm.

Alpine metamorphic zonation within these different subunits exhibits generally increasing metamorphic grade in a southeastward direction. Though, apart from local zones of high strain (e.g. shear zones), the extent of Alpine deformation in this segment of the Austroalpine basement is not well defined, it is generally clear that eventual penetrative Alpine structures were formed rather early with respect to the thermal evolution; most fabrics from higher greenschist or amphibolite grade regions document an episode of static crystallization, hardly influenced by later stages of deformation during decompression and cooling. The most conspicuous feature of this crystallization, also referred to as "thermal climax" (THÖNI, 1983), is the post-kinematic growth of higher grade minerals, like garnet and staurolite (HOINKES, 1981; HOINKES et al., 1987). The timing of this important evolution stage of the eo-Alpine cycle was placed close to 90 Ma for the study area (see Figs. 11, 12 for review), but for other parts of the Austroalpine domain a significantly earlier onset of the cooling process was postulated on the basis of radiometric evidence (e.g. STÖCKHERT, 1984; OBERHÄNSLI et al., 1985; FLISCH, 1986; KRALIK, 1983; see also SATIR, 1975). This differential deformation and cooling raises new questions about the timing and, especially, the final stages of the first Alpine subduction-collision event.

The data in the present paper pose some new constraints on the eo-Alpine deformation history and, especially, on the timing of the detachment and thrusting of the Austroalpine basement nappes.

3. Penetrative Structures in the Southwestern Ötztal Unit

VAN GOOL, KEMME and SCHREURS carried out structural investigations along a ca. 40 km W–E traverse through the southern Ötztal basement (VAN GOOL et al., 1987). In this area, Alpine metamorphic grade increases continuously from ca. 300°C in the W to ≥600°C in the E (THÖNI & HOINKES, 1987, for review). The well-established zonation of eo-Alpine metamorphic temperatures seems to have been basically disrupted only at the southeasternmost end, close to the Periadriatic lineament, by a major tectonic line (called "Passeier line" in Fig. 2b; cf. KLEINSCHRODT, 1987).

VAN GOOL et al. (1987) discern structures relating to four different deformation phases (D_1–D_4). While not dealing with the first two (pre-Alpine) of them in this context, D_3 is of special interest, because it appears to be the last penetrative deformation, observed, though with varying intensity, all along the profile considered ("penetrative" is used here mainly as a regional term). D_3 is characterized as chevron type folding or kinking, with an axial plane foliation (S_3), however, occurring only rarely. The assumption that D_3 structure elements were formed during one distinct deformation event over the whole area in question is hypothetical and is based only on morphological criteria. However, if this assumption is correct, D_3 structures could provide essential information concerning extent, style and timing of an eventual Alpine restructuration in this basement unit.

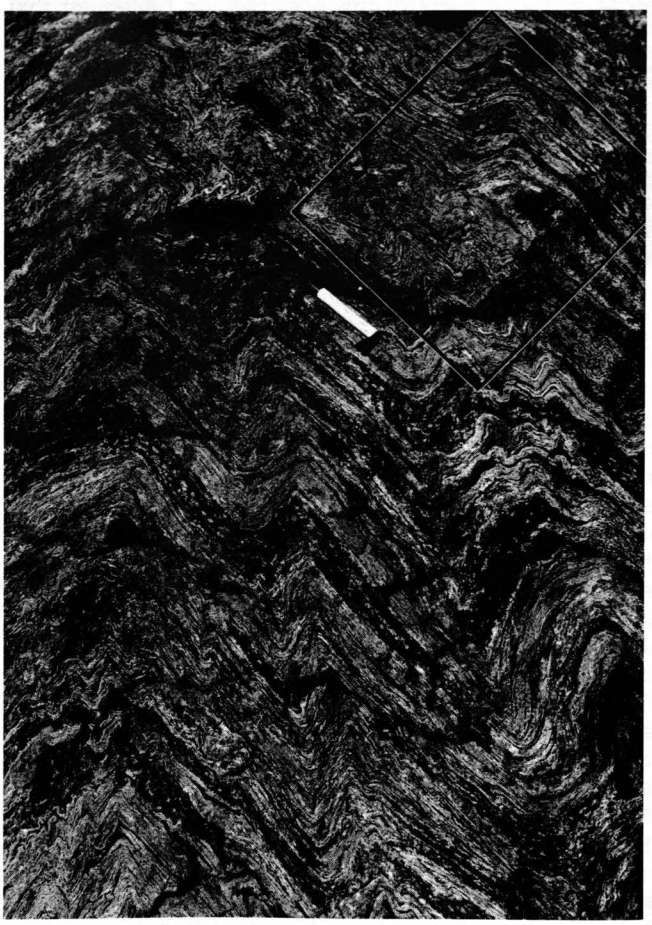

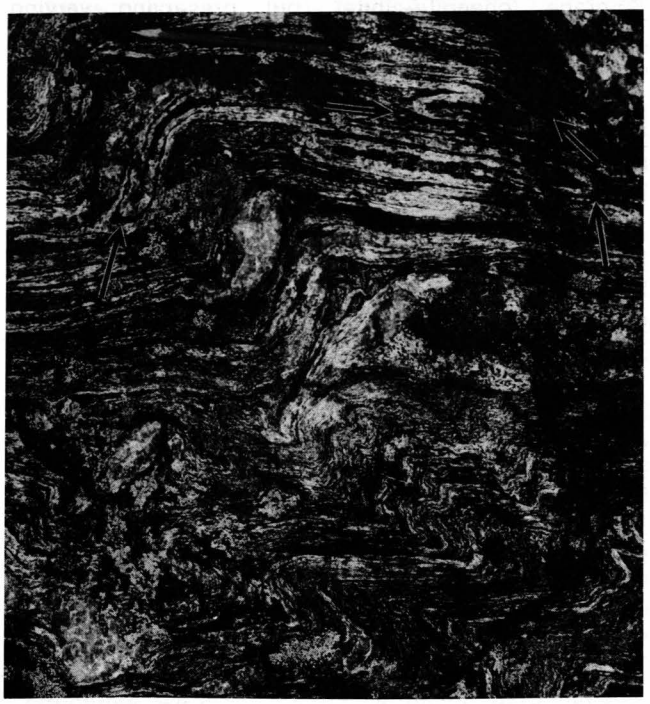

▲ b

◀ a

Fig. 4.
a) Typical appearance of asymmetric D_3 chevron folds with steep axial surfaces in layered paragneisses N of Weißkugel (loc. 1 in Fig. 2).
b) Detail from Fig. 4a (inset) showing refolding of small-scale D_2 isoclinal folds (arrows indicate hinges) by D_3 chevron folds..

3.1. D_3 Structures in the Weißkugel Area

Well-exposed outcrops in garnet-staurolite-kyanite-sillimanite-gneisses and micaschists in the uppermost valley of Langtaufers, some 4 km N of Weißkugel (Fig. 2), show clear overprinting relationships of at least three different deformation phases on the mesoscopic scale: the main foliation, as defined by the metamorphic microlayering is isoclinally folded (D_2 folds) and their axial planes are again refolded by D_3 tight or open folds, which frequently show steep axial planes. These latter structures are then cut discordantly by flat lying D_4 shear zones of varying dimensions (Figs. 4–6 and 15). From microscopic observations the following important conclusions are deduced for the relative timing of the crystallization/deformation history in these rocks.

1) D_2 folds formed in the ductile field for all constituent minerals. Crystallization of plagioclase, garnet and staurolite outlasted the D_2 event, as D_2 microfolds are in part clearly overgrown by cm-size porphyroblasts (Fig. 3).
2) D_3 folds formed at considerably lower temperatures, but cause little retrogression: micas are frequently kinked in the fold hinges of D_3 folds (Fig. 6b), but partly also synkinematically recrystallized (Fig. 6c); in some cases, a corresponding S_3 (axial plane) foliation is visible macroscopically (Fig. 5b).
3) D_4 structures are semiductile, they correlate with an intense retrogression of the higher grade mineralogy, resulting in a paragenesis of low- to very-low grade (phengite-albite), but preserving varying amounts of porphyroclasts (Figs. 10 and 16a).

3.2. Isotopic Results from D_3 Folds

D_3 folds reflect considerable strain, imposed in any case rather lately on a higher grade mineral assemblage. Their age has basic significance for the understanding of the Alpine evolution of the Austroalpine basement nappes, during their underthrusting, offshearing and tectonic transport. Reliable geochronological dating of D_3 fold structures may be expected to be difficult, as D_3-synchronous crystallization is rather limited. Using isotopic small scale results it should be possible, however, to decide, whether this deformation belongs to the pre-Alpine or rather to the Alpine cycle.

From the above described outcrops a two-mica-paragneiss (T1027), containing little garnet and sillimanite and showing typical D_3 structures (Fig. 6a,b) was analyzed by the Rb-Sr method. Plagioclase, white mica and biotite were separated from a kg size sample. Additionally, several biotite concentrates were gained from thin slices, cut approximately parallel to the axial planes of the D_3 folds, of the same specimen. Only one mineral generation (mm-size) is observed microscopically, and retrogresssion is restricted to occasional tiny chlorite rims around the coarse-grained biotite flakes. In order to study the influence of deformation, slices with and without strongly kinked portions were separated (hinges and limbs of cm-sized D_3 folds).

The Rb-Sr isotopic results are listed in Tab. 1 and plotted in Fig. 7. White mica, whole rock and plagioclase define an isochron age of 296 ±2 Ma (2σ). This figure is well in line with previously reported mineral ages of those parts of the Austroalpine basement that show very weak Alpine metamorphic overprinting (e.g.

▲ a

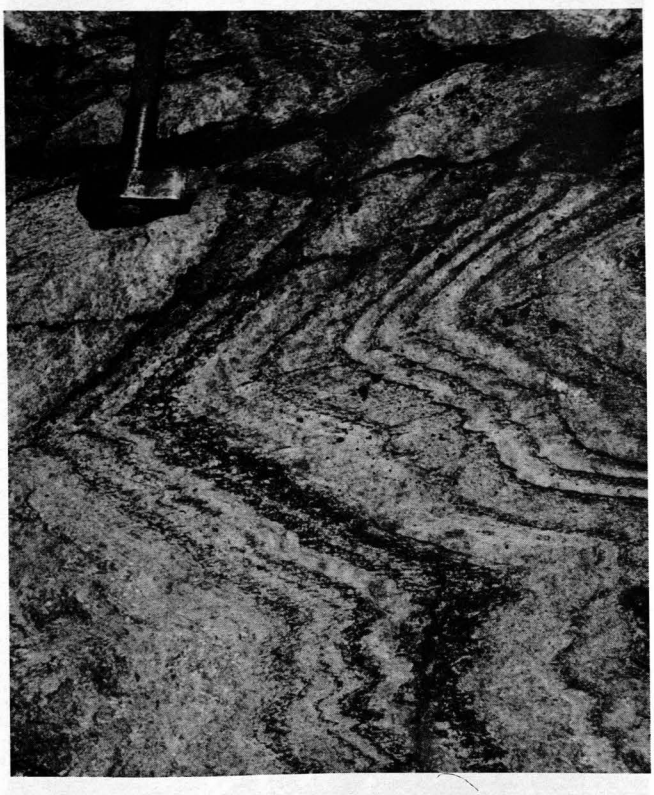

b ▶

Fig. 5.
a) Regular and symmetric dm–cm scale D_3 folds; arrows indicate zones where recrystallization of coarse mica is recognized macroscopically in the fold hinges; broken lines mark the trend of axial surfaces, along which an incipient axial plane foliation is developed.
b) In a few cases, like the present example, a more clearly developed axial plane foliation is observed within D_3 folds.

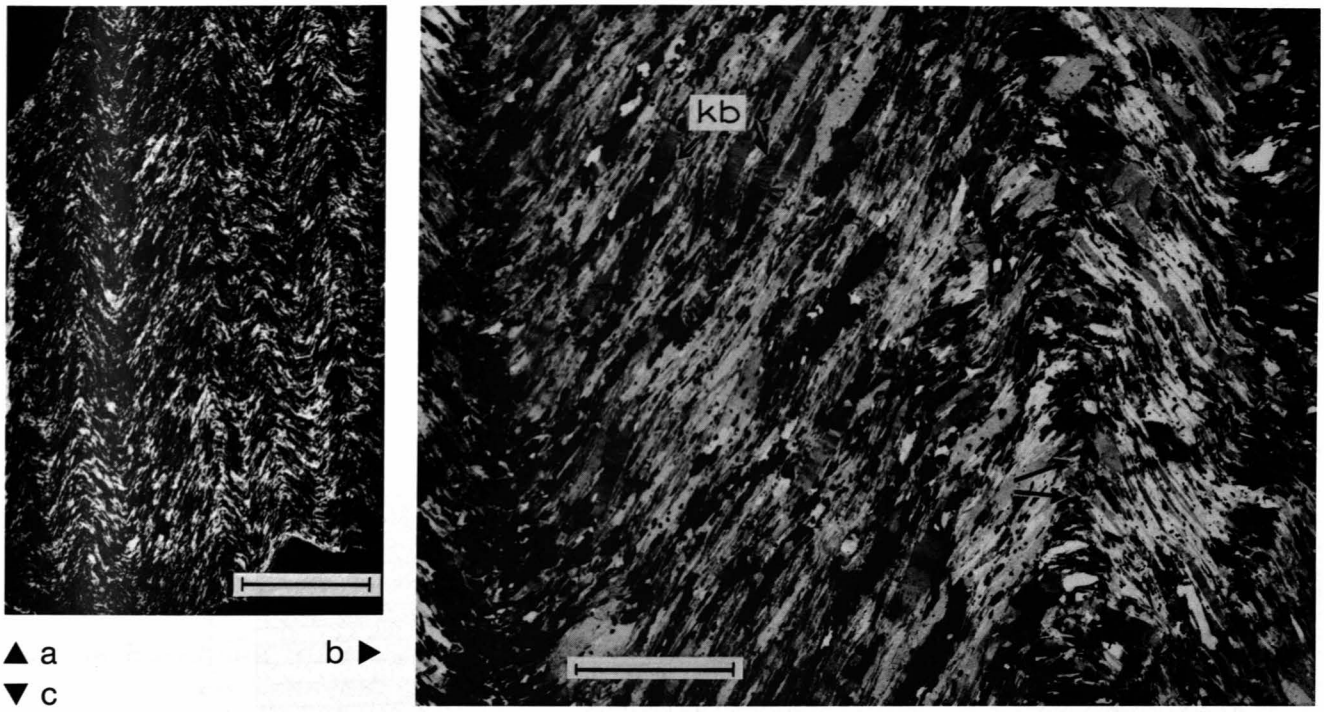

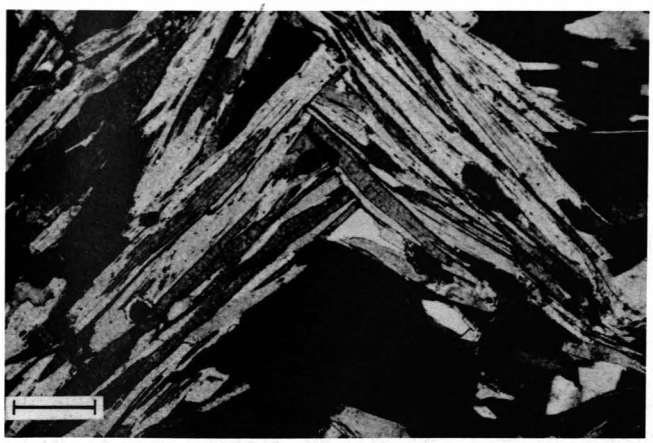

Fig. 6.
a) Polished specimen of sample T1027 as used for thin slab mineral analysis, showing D_3 structures on the cm scale.
Scale bar = 2 cm.
b) Thin section photograph of kinked paragneiss T1027 from N of Weißkugel. In this case, no axial plane foliation is developed, and the micas are only rarely recrystallized in the fold hinges (arrows, and Fig. 6c). The microkinks as observed within coarse biotite grains (Kb) in the fold limbs may be either of syn- or post-D_3 age.
Scale bar = 4 mm.
c) Detail from Fig. 6b showing coarse-grained recrystallization of biotite and white mica in a D_3 microfold hinge. Since Alpine metamorphic temperatures were definitely too low to recrystallize coarse mica in this area, pictures like these strongly argue against an Alpine age of D_3.
Scale bar = 0.2 mm.

GRAUERT, 1969; THÖNI, 1981) and is interpreted to reflect the end of the Hercynian crystallization.

As a mineral with rather low closing temperatures, biotite may be regarded as the most meaningful for our specific question. The two biotite concentrates as separated from the whole rock specimen give mineral – whole rock isochron age results of 258 ±2 (coarse) and 242 ±2 Ma (finer grain size), respectively. The biotites gained from the thin slabs (see Fig. 7, Tab. 1) range with their ages between 238 ±2 and 292 ±2 Ma, yielding a mean value of 265 Ma for twelve analyses.

Published Rb-Sr and K-Ar biotite ages from the study area, but derived mostly from samples that lack such an intense D_3 crenulation, cluster between 270 and 300 Ma (THÖNI, 1986, for review) with slightly lower age values occurring locally (unpublished data). It was argued therefrom that model ages of <ca. 270 Ma may signal first Alpine influence. The mean value of 265 Ma for the twelve biotite concentrates from sample T1027 lies thus at the lowermost limit of what is taken as undisturbed Hercynian age group. However, a weak later influence is recognizeable in the biotites of slabs 1–5, yielding model ages of 238–258 Ma. This slight Sr loss is hardly correlatable with any significant mineralogical or structural observations, except that grain-internal deformation (kinking) in slabs 1–5 seems to be somewhat more frequent than in the rest of the specimen.

Thus, although the isotopic results alone are not fully conclusive, they anyhow favour a Hercynian rather than an Alpine formation of the D_3 structures, in the present case. Apart from the ages, especially the fact that coarse-grained micas did partly recrystallize in the fold hinges in an otherwise equal-grained, monophase texture during the D_3 event supports a pre-Alpine formation of these structures (Fig. 6c). Alpine metamorphic conditions were definitely too weak to recrystallize coarse micas in this zone. If, on the other hand, the D_3 structures were a product of Alpine deformation, a more intense cataclastic destruction and more low-temperature strain effects in general would be expected for such a coarse grained paragenesis. About 30–50% of strain (shortening), as estimated from D_3 folds, would then have been accomodated in the rocks under largely dry (no retrogression) and very low-grade (subgreenschist facies) conditions. Since almost no secondary, strain-induced recrystallization is observed in thin section and crystal plasticity as well as pressure solution at such cool and "dry" environmental condi-

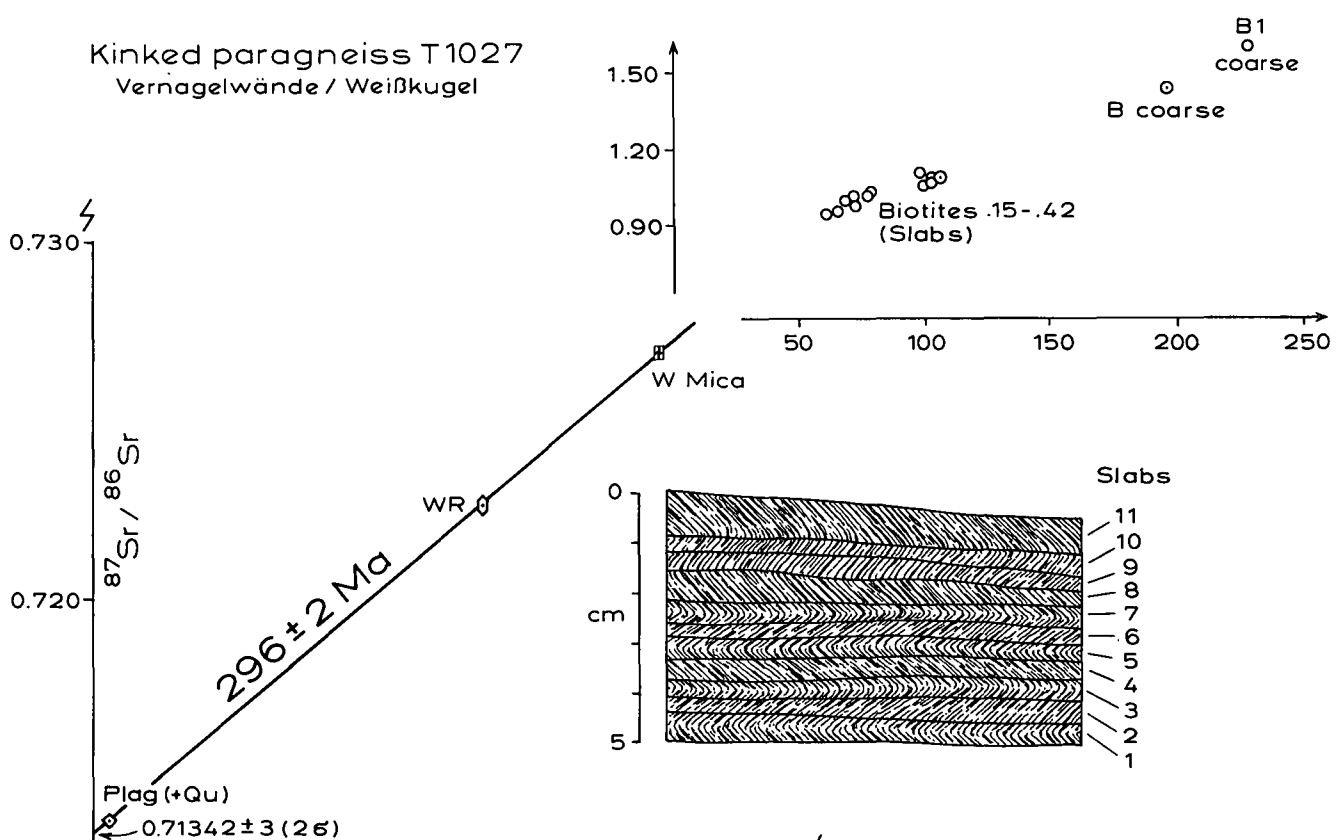

Fig. 7.
Rb/Sr evolution diagram for plagioclase (including quartz), white mica (W mica) and whole rock (WR) of paragneiss T1027.
The mineral-whole rock isochron ages corresponding to the 14 biotite data points as shown on the right upper part of the graph span the time interval of between 238 and 292 Ma, thus supporting a Late Hercynian rather than eo-Alpine age for the D_3 structures in the specimen analyzed.

Table 1.
Small scale Rb-Sr data on minerals of crenulated paragneiss sample T1027 (WAP 890, Vernagelwände/Weißkugel).

Analyzed material and grain size [mm]	ppm Rb	ppm Sr	$^{87}Rb/^{86}Sr$	$^{87}Sr/^{86}Sr \pm 2\sigma_m$	WR-Mineral Isochron Age [Ma]	
Whole rock (kg size)	217.6	287.3	2.202	0.72265±17		296±2
White mica (0.15–0.42)	228.7	207.5	3.205	0.72693± 9	300±12	
Plagioclase (+ quartz) (0.15–0.42)	13.82	436.5	0.092	0.71381± 5	294±10	
Biotite (>0.18)	419.7	6.66	196.0	1.43324±16	258± 2	
Biotite (0.15–0.42)	390.2	11.10	105.8	1.07867±16	242± 2	
Biotites from thin slabs (see Fig. 7)						
B 1 (0.15–0.42)	406.1	16.66	72.64	0.98010±13	257± 2	
B 1 (>0.18)	416.7	5.76	228.3	1.59853±20	272± 3	
B 2 (0.15–0.42)	380.7	11.07	103.3	1.06551±20	238± 2	
B 3 (0.15–0.42)	404.0	12.04	100.7	1.05640±25	238± 2	
B 4 (0.15–0.42)	400.8	11.66	103.3	1.06758±20	240± 2	
B 5 (0.15–0.42)	402.0	18.12	66.0	0.95698± 6	258± 2	
B 6 (0.15–0.42)	414.0	12.70	98.36	1.10489±24	279± 2	
B 7 (0.15–0.42)	397.9	17.03	69.76	0.99582±16	284± 3	
B 8 (0.15–0.42)	408.8	19.86	61.18	0.95314±12	275± 2	
B 9 (0.15–0.42)	412.8	15.79	78.16	1.01384±12	269± 2	
B 10 (0.15–0.42)	398.5	16.52	72.14	1.01298±20	292± 2	
B 11 (0.15–0.42)	419.1	15.86	79.03	1.02646±11	278± 3	

WR = whole rock; B = biotite.

tions were probably not very effective in most of the minerals, grain boundary sliding remains the only plausible deformation mechanism. An important question in this context concerns the strain rate (cf. PFIFFNER & RAMSAY, 1982), especially with respect of Sr-loss by diffusion. If D_3 folds formed within a long time span of, say, some tens of millions of years, loss of radiogenic Sr enhanced by lattice-internal deformation from least retentive minerals, like biotite, could well be significant, even if ambient temperatures reached hardly the conventional closing/opening conditions. At any rate, the preservation of unaltered Hercynian biotite ages in slabs 6–11 does not favour a strain-induced partial Alpine rejuvenation in the remaining biotites. In conclusion, structural as well as isotopic constraints support a Late Hercynian rather than an Alpine age for what have been characterized as D_3 structures in this southwestern part of the Ötztal unit.

4. D_3 Type Structures in the Eo-Alpine Staurolite-Kyanite Zone (Texel-Schneeberg Area) and the Question of Alpine Restructuring of the Basement

The question about the extent of deformations accompanying the eo-Alpine Schneeberg crystallization in the SE Ötztal and, more precisely, the question as to which structures are clearly of Alpine age, is rather difficult to answer. The following points should be stressed.

a) The mere fact that the rocks were metamorphosed in the ductile field and that general mobility (plasticity) was high is not a sufficient argument in order to correlate penetrative deformation structures straightforward with the last tectonothermal event.
b) Microstructural and textural evidence is insufficient in many cases for assigning an age to distinct structure elements; mineral orientations may follow preexisting (= pre-Alpine) structures, e.g. by paralleling pre-Alpine schistosity. Undoubtedly, in the ductile field (≥500°C), grain boundary sliding and plastic flow may have been active to a variable extent on the small scale, without, however, destroying older mesoscopic and macroscopic structures. In addition, on the (sub-)grain scale, small scale features are frequently overprinted by secondary grain growth (collective crystallization) and posttectonic (static) annealing.
c) Because of this relationship of (re-)crystallization and deformation and the argument put forward in chapter 1, a geochronological approach is even more difficult: most isotopic systems applied record, in this temperature range, only some stage of the cooling path or, at best, the last crystallization, but not the age of earlier deformations, with any reliability.
d) Permomesozoic sediments as found, e.g., in the Schneeberg area, reliably document the extent and style of the Alpine deformation. Marbles at this locality are ductilely deformed and stretched (cf. Fig. 8d). However, the parallelization of structure elements, in two such different rock series like the Permomesozoics and the polyphase basement is a difficult attempt and requires, first of all, detailed structural investigations. Because of the strongly different competence of these two rock sequences, deformation by sliding, shearing and thrusting is preferentially easy along the mutual contacts and is, in fact, observed extensively in the field (e.g. FRIZZO & CANALE, 1981).

Despite these facts and restrictions, many microstructural observations do at least strongly suggest an Alpine deformation within the basement that must, however, have been active rather early, when metamorphic temperatures were high. This is supported by the observation that microfolds and crenulation cleavages are "postkinematically" overgrown, e.g. by garnet and idiomorphic staurolite. The last penetrative mesoscopic structure elments observed in the eo-Alpine staurolite zone are crenulation cleavage folds, similar to the kink folds as described from the Weißkugel area. However, a crenulation cleavage is often extensively developed, microscopically defined by coarse mica flakes (Fig. 8). This crenulation cleavage, visible macroscopically in these rocks as second foliation, but with strongly varying intensity, might tentatively be interpreted as an Alpine structural element. The crenulation cleavage folds correspond to the D_3 structures of VAN GOOL et al. (1987). From regional considerations these authors came to the conclusion that D_3 folds are probably synchronous all along the traverse studied in the southern Ötztal unit; they were assigned to the pre-Alpine deformation history. Correspondingly, the important but rather implausible conclusion would result that almost no deformation accompanied the eo-Alpine metamorphism in this zone of the SE Ötztal unit, with rather high temperatures. In some places, however, coarse-grained mica sheets show undulous extinction in fold hinges of D_3 microfolds. This shows that deformation processes were active and partly even outlasted the eo-Alpine crystallization in this zone. Apart from deformation-induced recrystallization processes, like those active along the limbs of the crenulation cleavage folds, it is therefore documented, that pre-Alpine structure elements were at least reactivated (e.g. tightening of open chevron folds, etc.), if not newly formed, during the eo-Alpine tectonothermal event.

5. Pseudomorphosed Pre-Alpine Porphyroblasts from the Eo-Alpine Greenschist Facies Zone as Strain Markers

Important informations concerning the intensity and style of Alpine deformation arise from pre-Alpine porphyroblasts, such as staurolite, that were retrogressed during eo-Alpine thermal overprinting within the eo-Alpine metamorphic greenschist facies zone of the southern Ötztal unit (THÖNI & HOINKES, 1987).

Good outcrops can be studied near Oblatsch (at ca. 2800 m above S. L.), S of Eishof in Pfossental. This site is very close to the eo-Alpine staurolite-in boundary (about 2.5 km north of Texelsp. in Fig. 2a).

At this locality, large, cm-sized porpyhroblasts, partly still preserving an idiomorphic shape, are ob-

▲ a

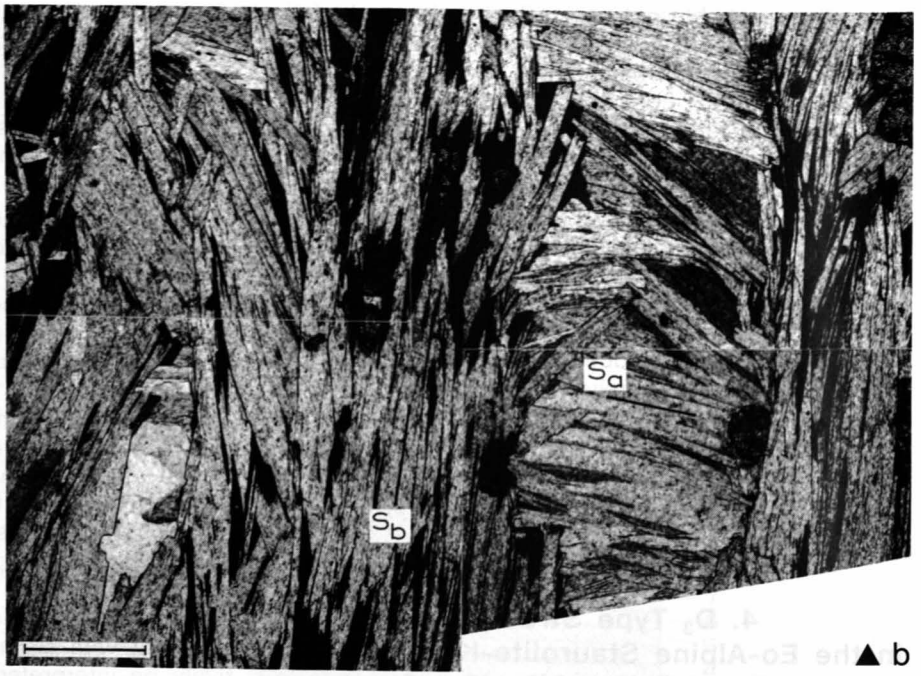

▲ b

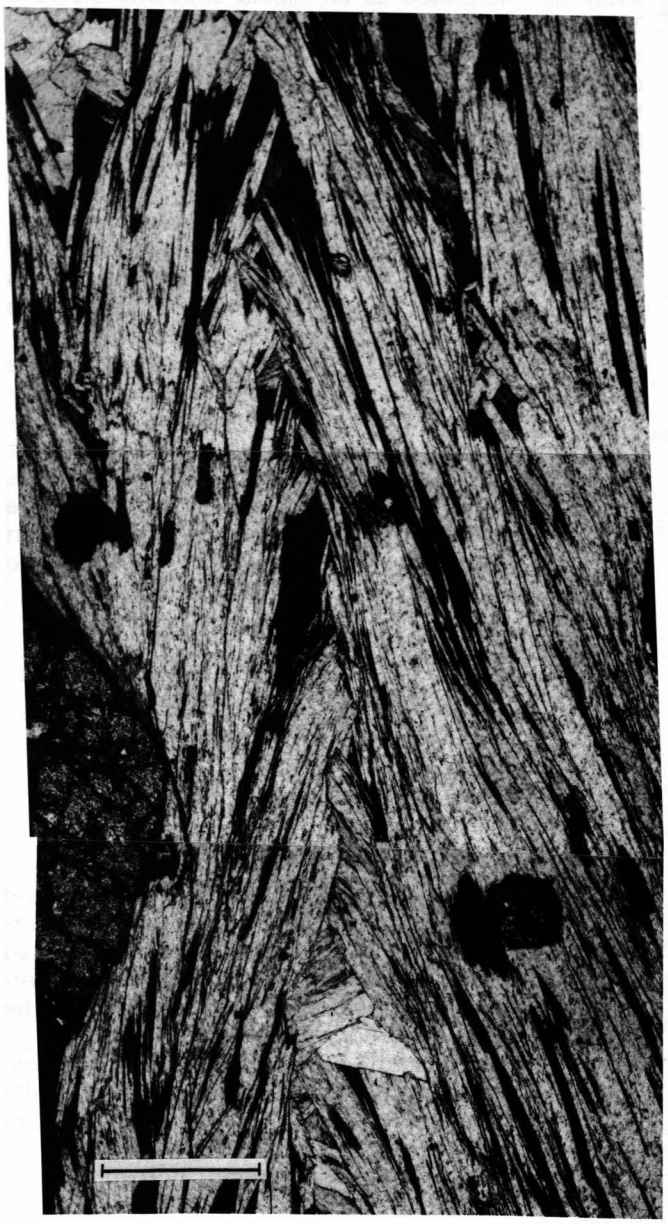

◀ c

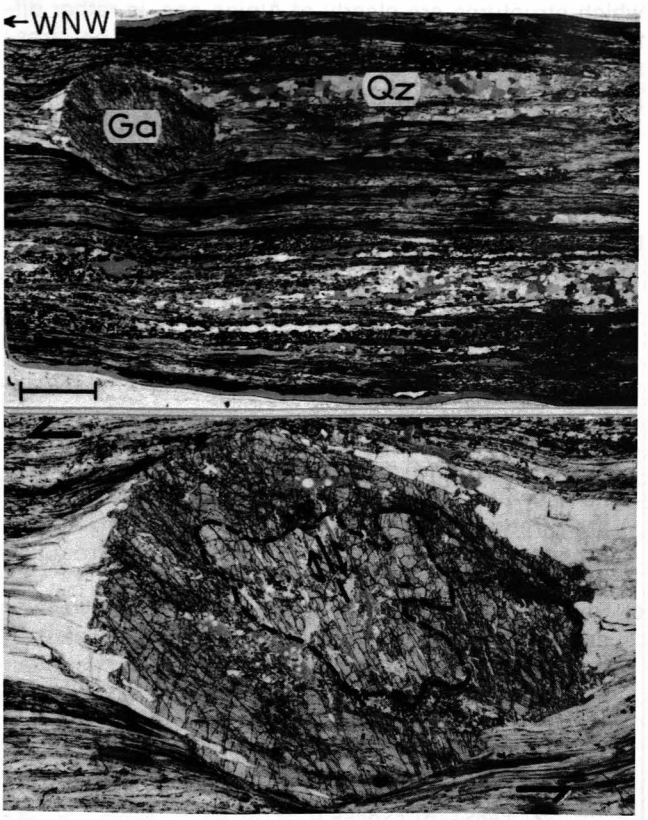

d ▲

served on the s-planes of garnet-micaschist; these blasts seem to overgrow the last lineation, as defined by the hinge zones of D_3 type crenulation cleavage microfolds (Fig. 9a). Under the microscope, the porphyroblasts appear as completely altered aggregates, composed of coarse, unoriented white mica that becomes finer grained towards the rims (Fig. 9b). The contacts of these pseudomorphs which probably represent retrograded pre-Alpine staurolite, are generally sharp and discordant relative to the external micaschist fabric, whose constituent minerals are mostly recrystallized. Weak imprints of later, clearly Alpine deformation are documented by undulous extinction and local kinking approximately parallel to the microfold hinges. From this relation of (re-)crystallization to deformation and mineral orientation of pseudomorphs and micaschist fabric it is concluded, that the microfolds, though weakly reactivated during the Alpine cycle, were formed before the retrogression of the large porphyroblasts took place and might hence be of pre-Alpine age.

A review of a number of samples through the Alpine greenschist facies zone reveals mostly similar relationships between deformation and recrystallization (e. g. Fig. 9d), but a few cases show different situations. One example of young deformation is shown in Fig. 9c, where a pseudomorph is structurally overprinted by Alpine kinks. An other example, shown in Fig. 10, exhibits a completely different texture for rocks involved in Alpine shear zones (see chapter 7.).

The following conclusions may be derived from these observations for a W-to-E section through the southern Ötztal basement.

a) Reliably documented penetrative (small-scale) deformation related to (eo-)Apine overprinting events is random and, in any case, subordinate compared with the pre-Alpine one (VAN GOOL et al., 1987).
b) Classification of structure elements following morphological and orientation criteria alone is probably not sufficient for distinguishing different deformation events. In the present case, D_3 type structure elements could well be of a different age (pre-Alpine in the W, partly eo-Alpine in the E). Within the more ductile, Alpine higher grade parts of the SE Ötztal unit they could include for instance, a considerable early eo-Alpine component, though hardly recognizeable as such because of homoaxial reactivation on the one hand and postkinematic thermal overprinting on the other.

On a regional scale, the Ötztal-Stubai complex shows a typical domed thermal structure, with clearly hotter conditions at the root compared with the frontal part of the nappe (THÖNI, 1986). It is important to mention here that large-scale gentle or open folds were recognized as Alpine structures at different sites (e.g. VAN GOOL et al., 1987). If effective on the km scale, such large-scale eo-Alpine folding and bending may be of considerable importance. In connection with a probably complex thermal evolution during initial exhumation and thrusting (see CHAMBERLAIN & KARABINOS, 1987; SHI & WANG, 1987) such large-scale structures may have contributed to and may even help to better explain both the "pre-Alpine" Schlingenbau (see VAN GOOL et al., 1987) as well as the characteristic eo-Alpine metamorphic zonation, e.g., by steepening and overturning of the more interior parts of the thrust slice (Schneeberg area and south thereof; Figs. 2 and 22) during rapid uplift and cooling.

6. Remarks on the Regional Metamorphic Evolution and the "Thermal Climax"

A rough sketch of the Alpine metamorphic zonation in the central western Austroalpine nappes shows strongly varying thermal overprint of the different subunits, with, however, a general increase of the metamorphic grade in a south-eastward direction (THÖNI, 1981). Some of the geologically important radiometric dates from this region are summarized in Fig. 11. Considering two areas with strikingly different Alpine metamorphic overprint, i. e. the Scarl unit (lowest greenschist facies) and the southeast Ötztal basement (Alpine staurolite and kyanite, cf. Fig. 2), the age patterns obtained exhibit some remarkable similarities (plots a and b in Fig. 11):

a) The eo-Alpine imprint ist dominant and very little post-Cretaceous influence is documented.
b) A first order concentration of ages is observed around 90–85 Ma for both areas.
c) Additionally, plot b in Fig. 11, representing the eo-Alpine staurolite zone, appears to be clearly thermally controlled, if interpreted according to the blocking temperature concept. The pattern implies that cooling from ≥550 to 300°C was accomplished within some 15 Ma or less.

Fig. 8.
a) Crenulation cleavage microfolds from the eo-Alpine staurolite zone, Texel area (near loc. C on Fig. 2). A younger schistosity is partly developed as axial plane foliation, defined by coarse mica (s_b).
b,c) Coarse-grained recrystallization in a crenulated garnet-staurolite-micaschist from the eo-Alpine staurolite zone (sample T1499, east of Kolbenspitze). Within the microfold hinges, the individual grains completely lack internal deformation. In Fig. 8 b clearly two schistosities are recognized (s_a, s_b).
Scale bar = 0.4 mm.
d) Photomicrograph of a mylonitized garnet-micaschist (T1480) sampled close to the northern, tectonized contact between Schneeberg complex and "Altkristallin" (some 4 km SW Schneeberg in Fig. 2a).
Contrary to the examples shown in Fig. 8b,c, the fabric is tightly planar, accompanied by a macroscopically visible WNW–ESE trending lineation. Late- to post-kinematic small-scale thermal overprint is exhibited by grain growth and annealing within the quartz (Qz) ribbons. A large garnet (Ga, upper left) shows subhedral, but slightly asymmetric shape that could tentatively be evaluated as shear sense indicator (top to the left).
The lower part of the photograph shows the internal structure of the garnet in more detail: a lighter core (?pre-Alpine relic; demarcated by the broken line) and a rim that clearly overgrows the micaschist fabric. Both core and rim are cut by a system of microfractures along which grain internal displacement (preferably opposite to the main sense of shear) has taken place (arrows). Following the microstructure, mylonitization must have interfered with, but not outlasted final coooling (ca. 80 Ma). This is well in line with earlier Rb-Sr data from a nearby locality (THÖNI, 1986).
Scale bar = 4 mm for upper part.

▲ a

▲ b

▼ c

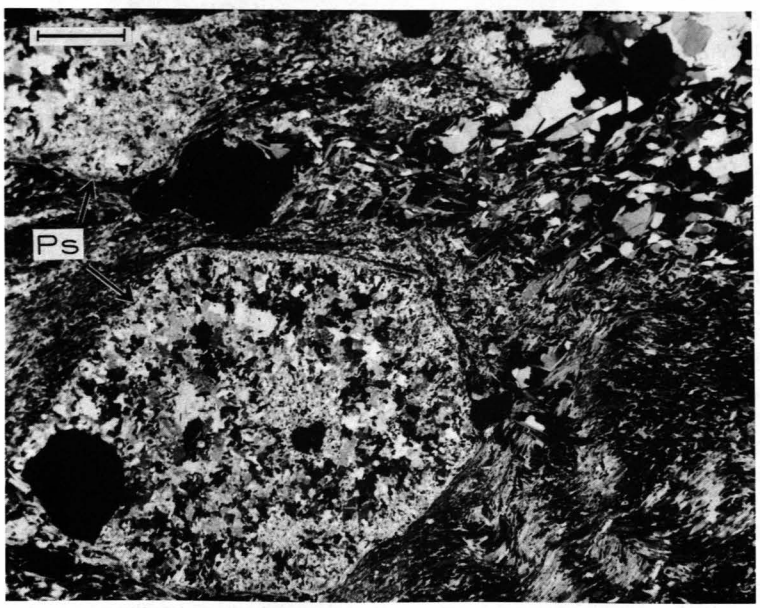

▼▼ d

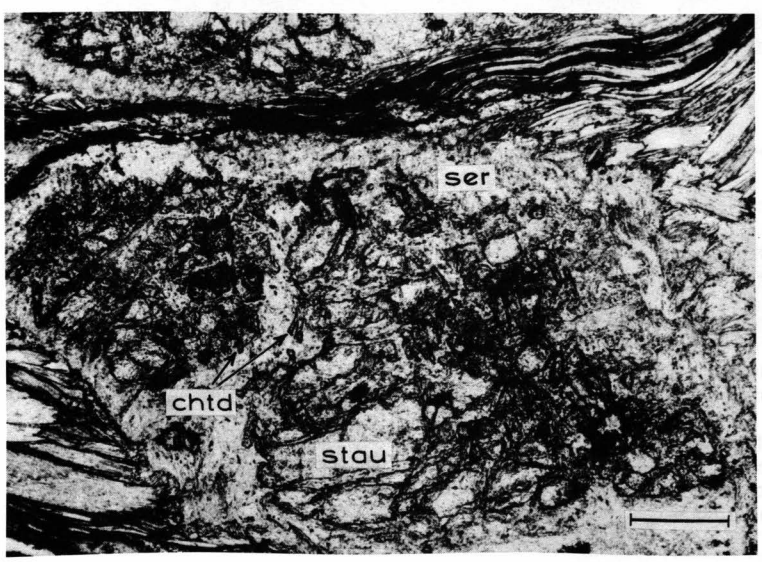

Fig. 9.

a) Crenulated garnet-micaschist T1223 with up to dm-sized pseudomorphs (ps), probably after pre-Alpine staurolite, that still partly show an idiomorphic shape. The lineation running approximately at right angles to the long side of the photograph marks the hinges of microfolds (see trend of broken line).

b) Photomicrograph of sample as shown in Fig. 9a.
A large idiomorphic pseudomorph (ps), composed of white mica shows no internal orientation of the constituent mica grains; the retrogression process may hence be younger than the crenulation observed in the external fabric.
Scale bar = 2 mm.

c) Intensely kinked micaschist from the eo-Alpine chloritoid zone, showing a pseudomorph, probably again after a pre-Alpine staurolite.
In this case, the kinks (k) that give an irregularly undulous appearance to the external fabric can be traced directly into the fine-grained mica of the pseudomorph, thus supporting an Alpine age for the kinks.
Sample T1590, near Gerstgras/Schnalstal (ca. 8 km W of Texelspitze, see Fig. 2).
Scale bar = 1 mm.

d) Example from the western part of the eo-Alpine chloritoid zone showing a pre-Alpine staurolite crystal, which is almost undeformed and preserved its idiomorphic rhomboidal shape, but was decomposed largely to fine-grained white mica (ser) and chloritoid (chtd), stau = relictic staurolite.
Despite of the rather frequent occurrence of microshear-bands (upper part of the photograph) and shear zones, prevailing patterns like these within the eo-Alpine greenschist facies zone, demonstrate that Alpine deformation was generally not penetrative in this part of the basement.
Sample T1054, near Steinschlagjoch, some 5 km SE of Weißkugel (see Fig. 2).
Scale bar = 0.3 mm.

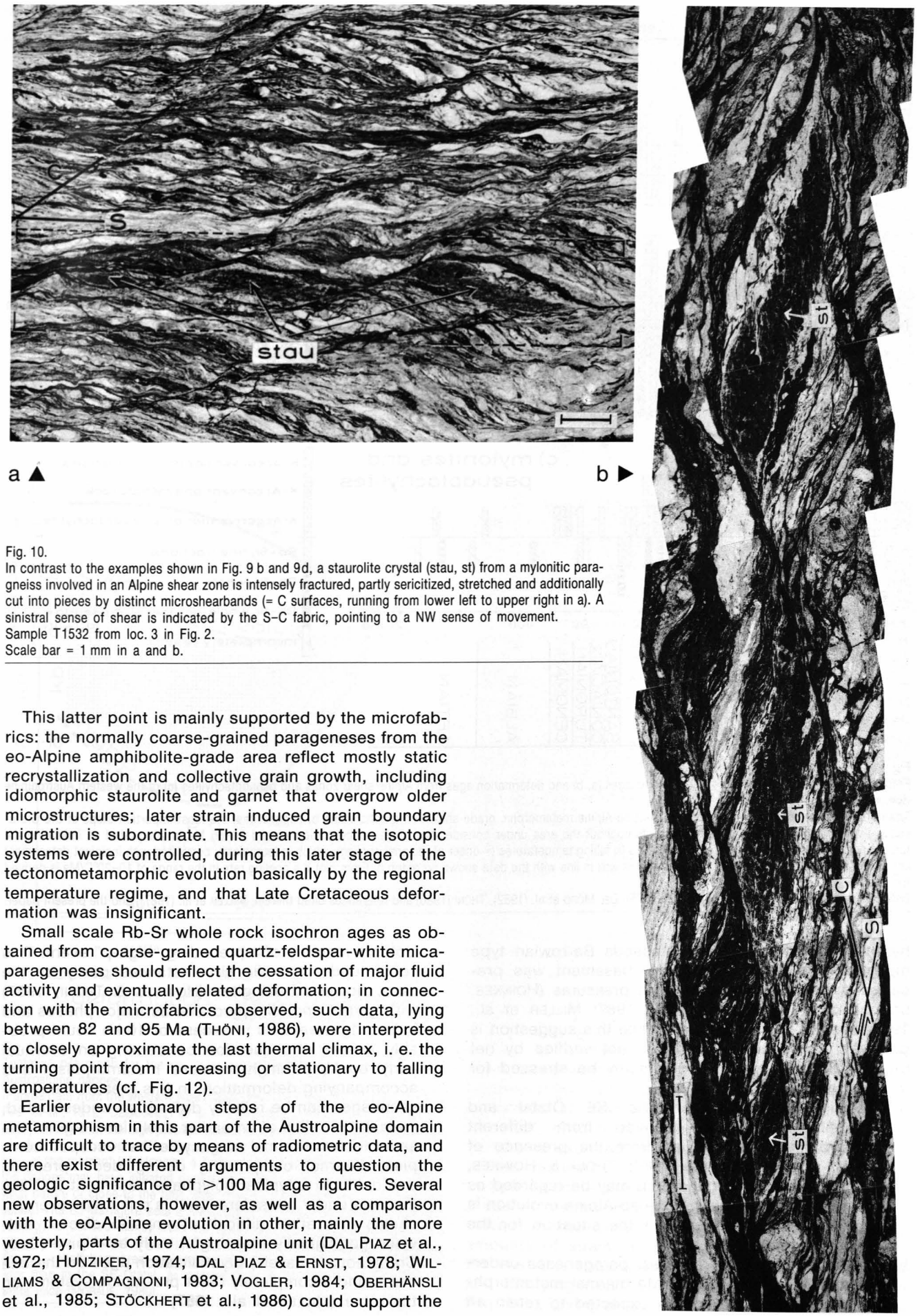

a ▲ b ▶

Fig. 10.
In contrast to the examples shown in Fig. 9 b and 9d, a staurolite crystal (stau, st) from a mylonitic paragneiss involved in an Alpine shear zone is intensely fractured, partly sericitized, stretched and additionally cut into pieces by distinct microshearbands (= C surfaces, running from lower left to upper right in a). A sinistral sense of shear is indicated by the S–C fabric, pointing to a NW sense of movement.
Sample T1532 from loc. 3 in Fig. 2.
Scale bar = 1 mm in a and b.

This latter point is mainly supported by the microfabrics: the normally coarse-grained parageneses from the eo-Alpine amphibolite-grade area reflect mostly static recrystallization and collective grain growth, including idiomorphic staurolite and garnet that overgrow older microstructures; later strain induced grain boundary migration is subordinate. This means that the isotopic systems were controlled, during this later stage of the tectonometamorphic evolution basically by the regional temperature regime, and that Late Cretaceous deformation was insignificant.

Small scale Rb-Sr whole rock isochron ages as obtained from coarse-grained quartz-feldspar-white mica-parageneses should reflect the cessation of major fluid activity and eventually related deformation; in connection with the microfabrics observed, such data, lying between 82 and 95 Ma (THÖNI, 1986), were interpreted to closely approximate the last thermal climax, i. e. the turning point from increasing or stationary to falling temperatures (cf. Fig. 12).

Earlier evolutionary steps of the eo-Alpine metamorphism in this part of the Austroalpine domain are difficult to trace by means of radiometric data, and there exist different arguments to question the geologic significance of >100 Ma age figures. Several new observations, however, as well as a comparison with the eo-Alpine evolution in other, mainly the more westerly, parts of the Austroalpine unit (DAL PIAZ et al., 1972; HUNZIKER, 1974; DAL PIAZ & ERNST, 1978; WILLIAMS & COMPAGNONI, 1983; VOGLER, 1984; OBERHÄNSLI et al., 1985; STÖCKHERT et al., 1986) could support the

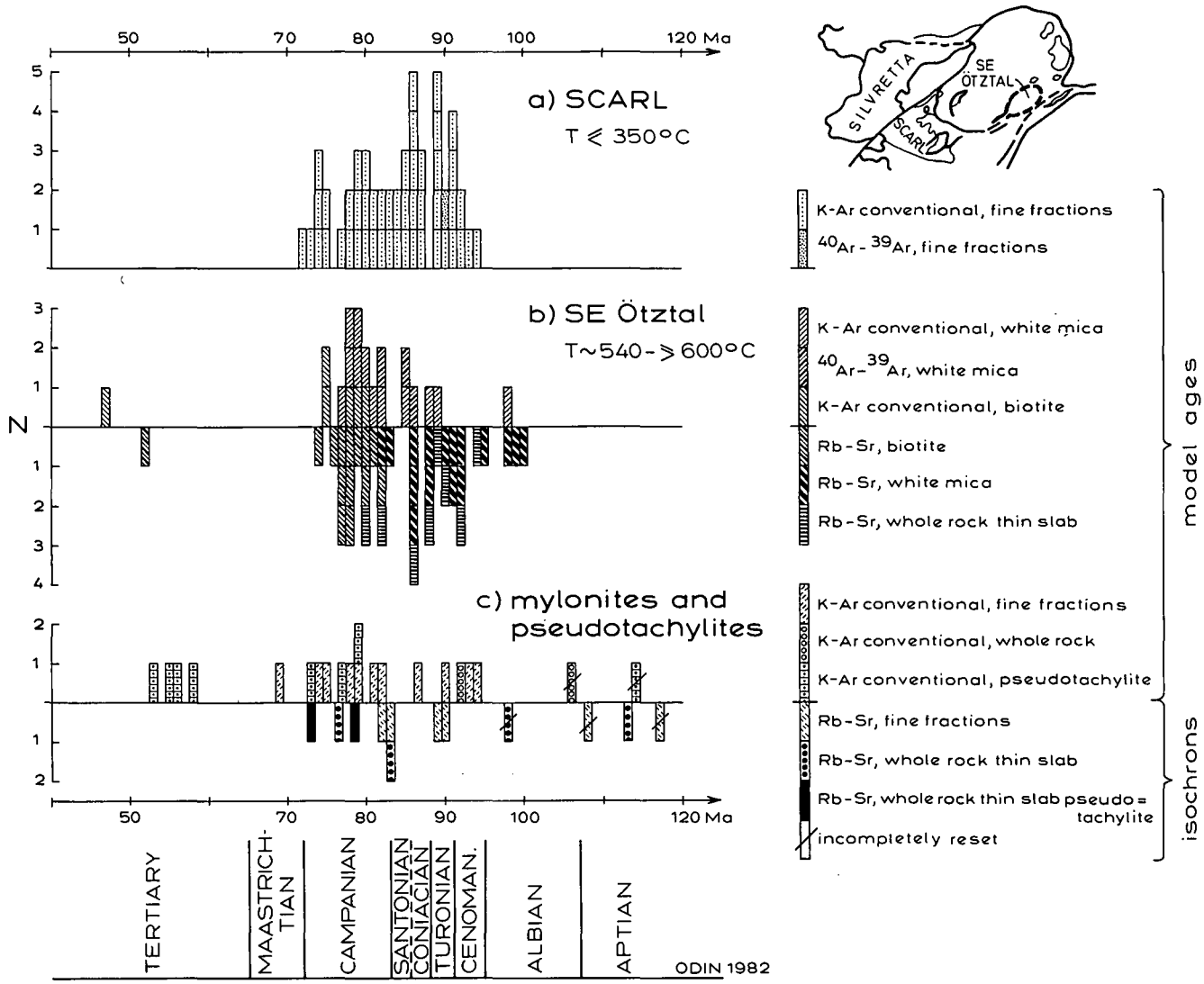

Fig. 11.
Frequency distribution of eo-Alpine metamorphic ages (a, b) and deformation ages from Alpine shear zones and pseudotachylites (c) of the western Austroalpine domain (for localities see Fig. 2).
The data from two areas with strikingly different eo-Alpine metamorphic grade shown on graphs a and b, suggest that the most important steps of the Cretaceous thermal evolution were broadly coeval throughout the area under consideration. Data concentration around 90–85 Ma is interpreted as indicating the turning point from rising or constant temperatures to falling temperatures (= onset of regional cooling), which is tectonically correlated with incipient detachment and thrusting of the basement nappes. This view is well in line with the data shown on graph c. From plot b a cooling rate in the range of 10–20°C/Ma is derived for the time 90–75 Ma B.P.
Data taken from SCHMIDT et al. (1967), SATIR (1975), DEL MORO et al. (1982), THÖNI (1986) and references cited therein, MILLER et al. (1987), and the present paper.

hypothesis that the Late Cretaceous Barrowian type metamorphism in the SE Ötztal basement was preceded by a phase of rather high pressures (HOINKES, unpubl. data, HOINKES & THÖNI, 1987; MILLER et al., 1987; see loc. "C" in Fig. 2a). While this suggestion is open for speculation as long as not verified by net radiometric evidence, two points my be stressed for the moment.

a) Pressure estimates for the SE Ötztal and Schneeberg unit as derived from different geobarometers as well as from the presence of kyanite (HOINKES et al., 1987; THÖNI & HOINKES, 1987) and ranging around 6 kb may be regarded as minimum values if the whole eo-Alpine evolution is considered. They only reflect the situation for the Late Cretaceous.
b) Similarly as for the pressures, parageneses undergoing a quite severe <100 Ma thermal metamorphism could generally not be expected to retain an isotopic memory of a preceding "high-p" event. This could, under specific circumstances partly be the case, however; eclogites (HOINKES & THÖNI, 1987) with garnet and clinopyroxene as major phases and indicating pressures in excess of 10 kb could probably answer the question concerning an eventual early eo-Alpine high-pressure metamorphism and accompanying deformation, in this area, if these assemblages can be reliably defined as undestructed, metastable relics of an earlier evolution stage of the same tectonothermal megacycle that escaped complete thermal overprinting during decompression and uplift. In a typical polyphase basement unit like the area under consideration this point, however, includes the rather difficult attempt to discern between geologically meaningful early eo-Alpine (Early Cretaceous-Jurassic) crystallization ages on the one hand, and incompletely reset pre-Alpine systems on the other (MILLER et al., 1987).

A tentative pTt path including the new data from the westernmost parts of the Austroalpine domain (e. g. DAL PIAZ et al., 1972; OBERHÄNSLI et al., 1985) is schematically shown in Fig. 12.

In comparing the data just discussed with the spectrum of ages as gained from white mica-rich fine fractions of the weakly metamorphic Permomesozoic sequence from the Scarl unit (plot a in Fig. 11), it is striking that the model ages embrace essentially the same time span as the ones shown on plot b. Values close to 90 Ma stem from the weakest metamorphic parts and were tentatively interpreted as formation (= crystallization) ages related to the eo-Alpine thermal peak (THÖNI, 1981). The lack of >100 Ma model ages in general and the lack of relict isotopic domains in a 90 ±1 Ma ^{40}Ar–^{39}Ar plateau from a neogenic white mica of a moderately deformed Verrucano sample in detail (MILLER et al., 1987) strongly supports the conclusion that the main Alpine crystallization event did at least clearly outlast or is younger than 100 Ma, in this area. In this context, the question of whether the onset of regional cooling is strongly heterochronous in different weakly metamorphosed parts of the Austroalpine domain (cf. FLISCH, 1986; KRALIK, 1983) is of basic interest. Evidently, more ^{40}Ar-^{39}Ar data from neogenic Alpine minerals are needed to solve this problem.

In summary, the figure 90 ±5 Ma seems to mark in any case an important step of the Cretacous metamorphic evolution in this part of the Austroalpine units. Extensive detachment and the initiation of thrusting of the nappes, following a supposed Mid-Cretaceous continental collision, could account for, as one possible explanation, the uniform interruption of the prograde thermal evolution during Cenomanian–Turonian times.

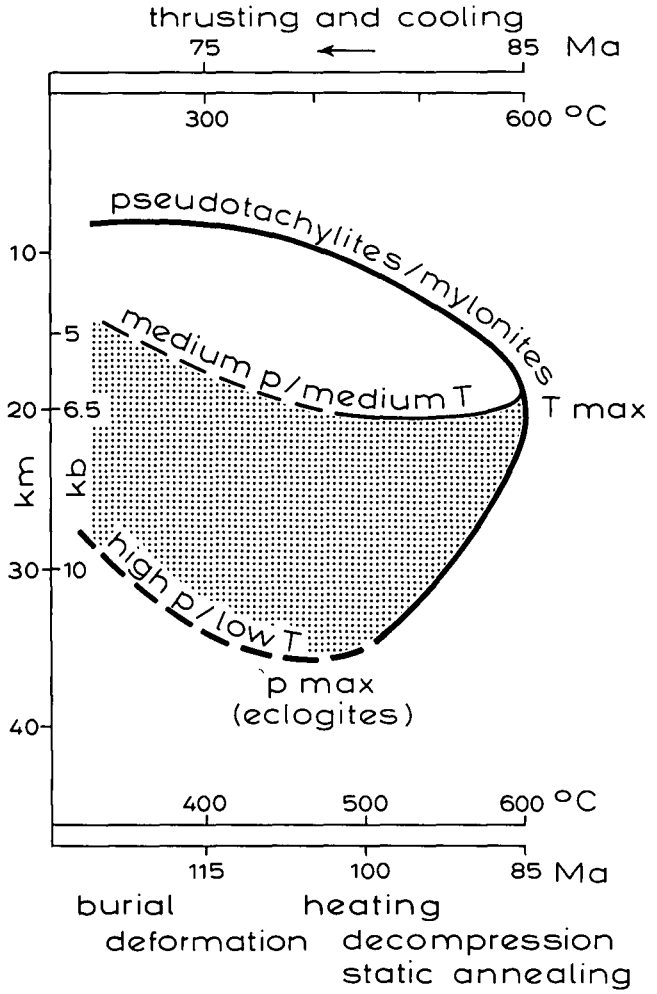

Fig. 12.
Tentative pTt graph for the eo-Alpine tectonometamorphic evolution of the Austroalpine nappes.
If some data from the western Alps (Sesia zone, Dent Blanche nappe; e.g. DAL PIAZ et al., 1972; OBERHÄNSLI et al., 1985; VOGLER, 1984; STÖCKHERT et al., 1986) are icluded, the high p/low T situation as shown on the lower half of the graph is proven, whereas for the area under investigation it is only speculative, at the moment (cf. HOINKES & THÖNI, 1987). Detachment and thrusting of the nappes may have initiated during exhumation and decompression, somewhat before or close to the time when maximum temperatures (T_{max}) were reached. The 85 Ma figure sets a lower age limit for the beginning of regional cooling, as derived mainly from the closing of geochronological systems in higher grade areas (cf. Fig. 11). In the eastern part of the Eastern Alps (e.g. Koralm - Wolfsberg area) regional cooling might have begun still somewhat later than in the SE Ötztal, as derived from Rb-Sr ages on coarse-grained white mica (MORAUF, 1980).

7. Post-D_3 Shear-Zones – Evidence for Eo-Alpine Detachment and Thrusting

Discordant shear zones of varying dimensions range among those structures that may be clearly assigned to the post-Hercynian deformation history. A considerable number of such zones of intense late deformation were discovered recently mainly in the southern Ötztal basement. Generally, these shear zones are flat lying or dip gently to the S or E. The rocks in these zones exhibit mylonitic fabrics, ranging from semibrittle to ductile. Often typical fluxion structures are recognizeable macroscopically. Different shear sense criteria, including mica fish, S-C fabrics (LISTER & SNOKE, 1984; BERTHÉ et al., 1979), prophyroclast rotation, bookshelf sliding (SIMPSON & SCHMID, 1983; SIMPSON, 1985; PASSCHIER & SIMPSON, 1986; RAMSAY & HUBER, 1987), etc. point to E (S) over W (N) movement (Figs. 13, 14). Although the suitability of such shear sense criteria for the reconstruction of large scale flow is partly questioned (e. g. BEHRMANN, 1987), some of these observations provide important informations concerning the kinematics of Alpine nappe tectonics. In connection with the age data to be discussed below, the data fit best with kinematic models as proposed recently for the early evolution steps of the Austroalpine nappes (RATSCHBACHER, 1986). The examples described in the following concern mainly the age relations as well as some general problems encountered in dating such shear zone rocks.

The Schlinig thrust (SCHMID & HAAS, 1987) is now known as a major intra-Austroalpine displacement zone, along which NW to W thrusting (Fig. 14a) of the southwestern Ötztal basement over the Scarl unit is proven for at least some 40 km. Whereas in the westernmost, brittlely deformed part (Schlinig) the thrust surface is exposed as a well mappable tectonic line, further eastwards (Vinschgau area) it develops into a complex ductile shear zone. Over at least some hundreds of meters across strike different lithologies involved in the shear zone exhibit strongly variable amounts of strain. In the higher-grade parts towards the east this zone displays frequently a very constant and flat-lying WNW–ESE trending stretching lineation (Fig. 14b), giving clear indication for penetrative ductile

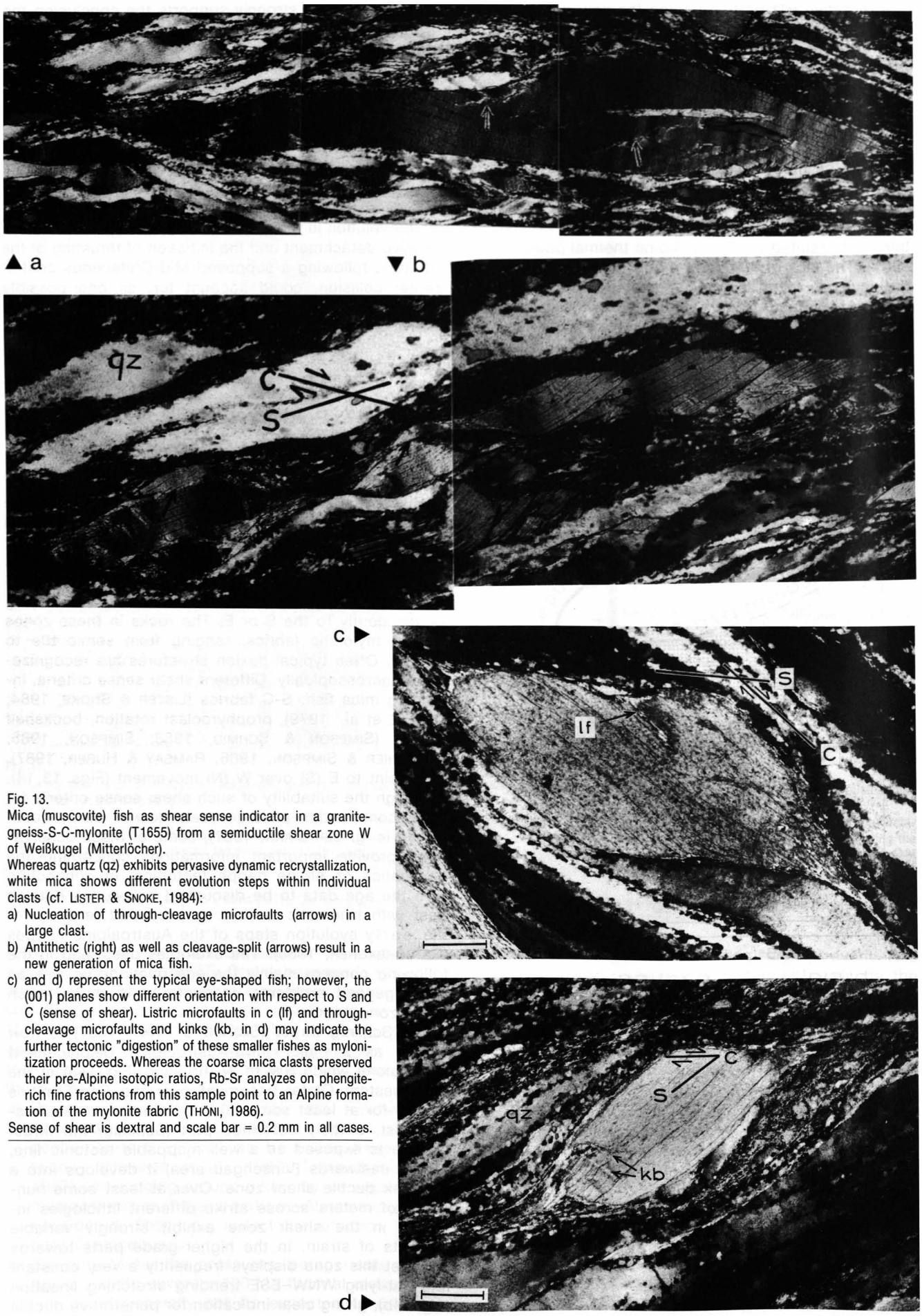

Fig. 13.
Mica (muscovite) fish as shear sense indicator in a granite-gneiss-S-C-mylonite (T1655) from a semiductile shear zone W of Weißkugel (Mitterlöcher).
Whereas quartz (qz) exhibits pervasive dynamic recrystallization, white mica shows different evolution steps within individual clasts (cf. LISTER & SNOKE, 1984):

a) Nucleation of through-cleavage microfaults (arrows) in a large clast.
b) Antithetic (right) as well as cleavage-split (arrows) result in a new generation of mica fish.
c) and d) represent the typical eye-shaped fish; however, the (001) planes show different orientation with respect to S and C (sense of shear). Listric microfaults in c (lf) and through-cleavage microfaults and kinks (kb, in d) may indicate the further tectonic "digestion" of these smaller fishes as mylonitization proceeds. Whereas the coarse mica clasts preserved their pre-Alpine isotopic ratios, Rb-Sr analyzes on phengite-rich fine fractions from this sample point to an Alpine formation of the mylonite fabric (THÖNI, 1986).

Sense of shear is dextral and scale bar = 0.2 mm in all cases.

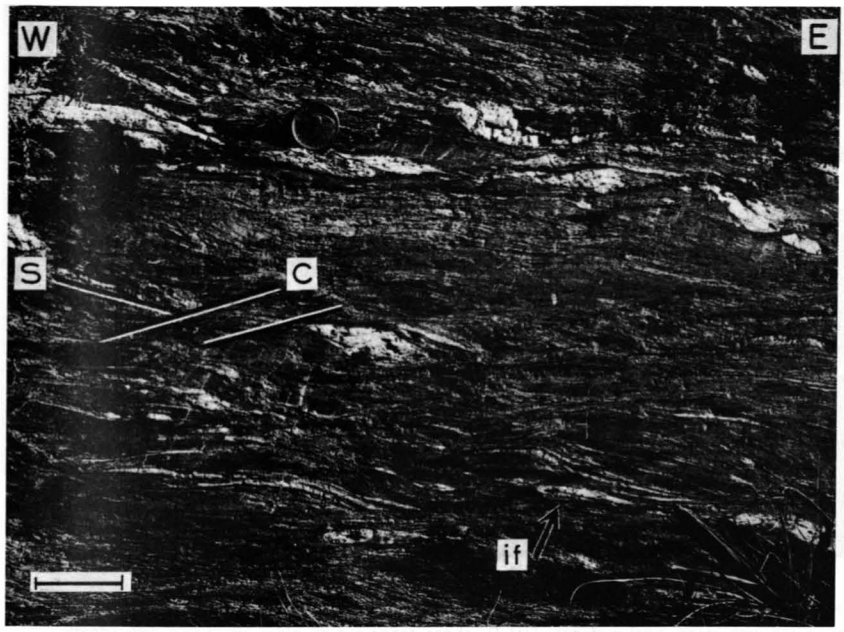

◀ a

b ▼

Fig. 14.
a) Mesoscopic S-C fabric in phyllitic quartz-mica-schist from the Schlinig thrust. Additionally, intrafolial folds (if) are observed.
K-Ar and Rb-Sr mineral and whole rock small-scale data from mylonitic rocks from this outcrop and surroundings cluster around 80±5 Ma; in connection with the structural observations these data point to a top E over W (left, bulk sense of shear is sinistral in the present case) thrusting during eo-Alpine cooling.
Loc.: Near Tappeinhof, Vinschgau (W of loc. 5 in Fig. 2).
Scale bar = 5 cm.
b) WNW–ESE trending stretching lineation in a mylonitic orthogneiss – another example for a dominant westward rock flow along the Schlinig thrust zone.
Loc.: Near Eyrs/Vinschgau, some 20 km W of loc. 5 in Fig. 2.

flow and, on a regional scale, to the movement direction of the nappes (cf. SHACKLETON & RIES, 1984). Since the different smaller shear zones from within the Ötztal basement complex (e. g. around Weißkugel, Fig. 15) show generally the same orientation and structural characteristics, they might well be regarded as syngenetic counterparts of the Schlinig thrust, related to a general westward movement of the nappes.

Some typical examples are described in the following and their age relations discussed. The corresponding sample localities are labelled 1–5 in Fig. 2. Sr isotopic analyzes of samples T1521 and T1631 have been reported previously (THÖNI, 1986).

❶ The first example stems from the outcrops described above from the Weißkugel area (Fig. 2), a zone with very low Alpine metamorphic grade. Here, narrow, flat lying shear zones cut older structures clearly discordantly, as shown in detail in Fig. 15. Within these zones of high strain, the coarse-grained paragneiss assemblage is extensively destructed to a very fine-grained, optically hardly resolvable material. Porphyroclast asymmetry and S-C fabric indicate northwestward sense of movement. A WNW–ESE to NW–SE trending stretching lineation is also developed. Field observations also support the conclusion that intense microfracturing may have accompanied or preceded ductile shearing, thus promoting fluid flux and localized deformation softening and, in turn, retrogressive reactions, resulting in the development of a new tectonic microlayering.
From a ca. 3 cm section of sample 86T19 (WAP 1388) that shows visible macroscopic microlayering the fine fractions <5 μ from eight layers were analyzed. The data points in the Rb/Sr evolution diagram (Fig. 16b) are arrayed along two trend lines with markedly different slopes, corresponding to age values of 82 Ma (layers 1–4) and 117 Ma (5–8), respectively. The spread in Rb/Sr is, however, rather small. Although these values give ample evidence for the Alpine age of the shear zones, the two regression ages shown should not be regarded as to indicating the exact time of deformation, as there is no microstructural evidence for such a divergence of the deformation process in time. Layers 5–8 represent the outer parts of the shear zone and are characterized by the presence of a higher proportion of porphyroclasts: hence the 117 Ma figure could be regarded as incompletely reset (meaningless or maximum) age, due to the contribution of inherited Sr from the porphyroclast material, whereas the 82 Ma figure could tentatively be interpreted as minimum age for the mylonitization process.

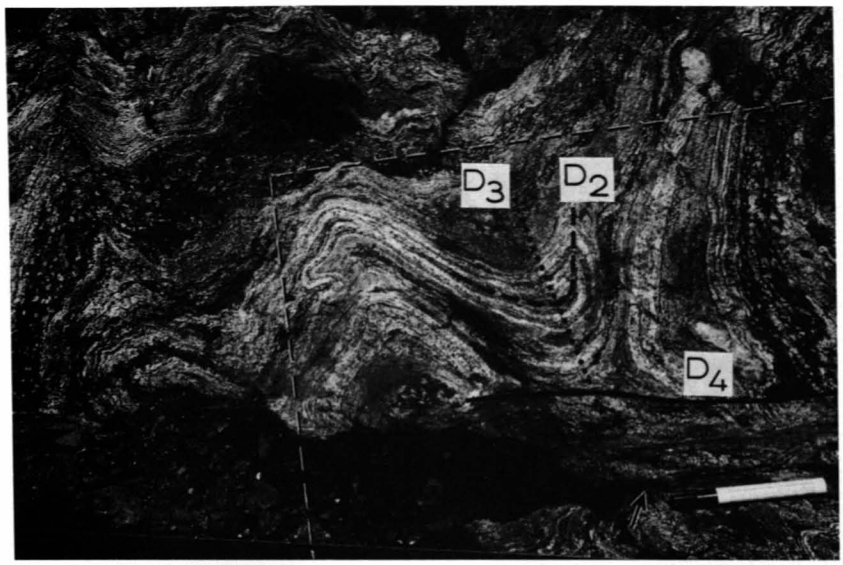

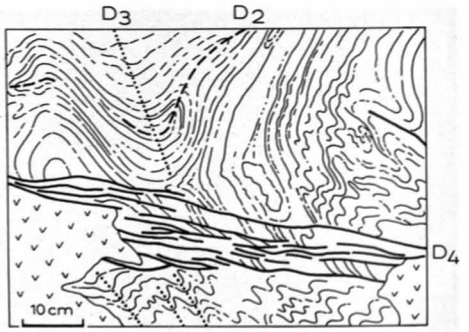

▲ b

◀ a

Fig. 15.
D_2, D_3, D_4 overprinting relationship in the polymetamorphic paragneisses N of Weißkugel.
The axial plane of D_2 isoclinal folds is refolded by D_3 structures with steep axial surfaces. Flat D_4 shear zones cut all older structures discordantly.
Arrow indicates sample locality of mylonite 86T19 (see Fig. 16a,b). Broken line marks inset of sketch (b).

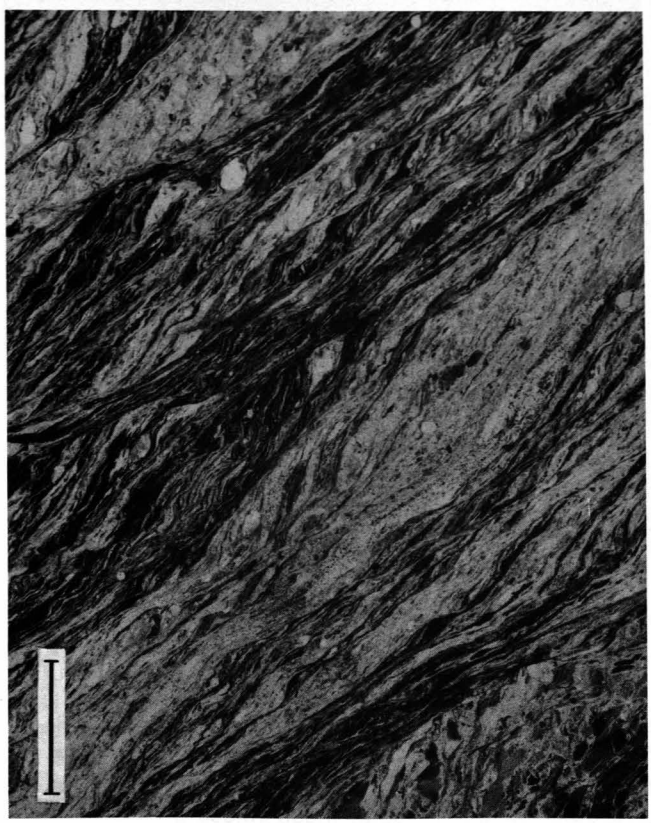

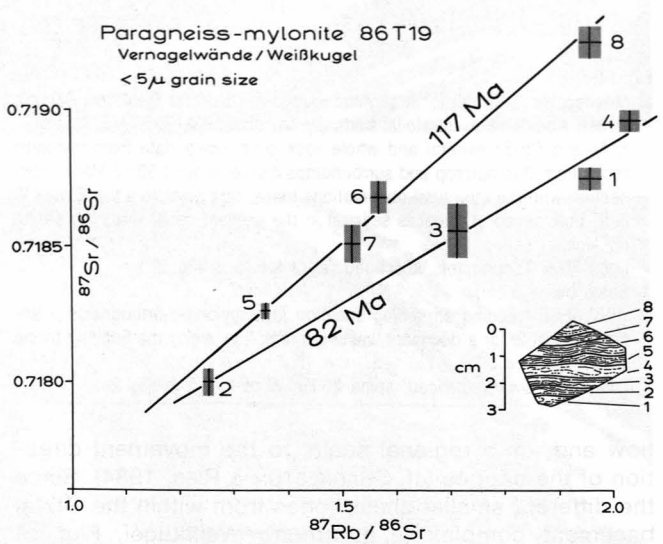

▲ b

◀ a

Fig. 16.
a) Photomicrograph of mylonite 86T19 showing microlayering, tectonic grain size reduction and S-C fabric.
Shear sense criteria permit, in connection with a weakly developed stretching lineation, derivation of a WNW directed movement in these outcrops. Note that the same sense of displacement prevails along the more significant Schlinig thrust zone (cf. Fig. 14a,b).
Scale bar = 2 mm.
b) Rb/Sr evolution diagram of fine fractions (<5 μ) separated from thin slices (microlayers) of mylonite 86T19.
Whereas the 117 Ma figure relates to the outer parts of the specimen (i.e. towards the undeformed country rock) and is interpreted as incompletely reset system, the 82 Ma regression age may be regarded as the minimum age for the mylonitization process.

❷ Example no. 2 (M230) was collected by M. KEMME (see VAN GOOL et al., 1987) W of Kurzras in Schnalstal, some 5 km SSE of Weißkugel, a locality lying well within the lower grade Alpine greenschist facies zone. The sample was taken from a quartz mylonite zone reaching several meters in thickness. On the (sub-)cm scale, ist shows a rather well-recognizable microlayering, defined by different amounts of quartz, white mica and fine-grained plagioclase. It is most important to note that white

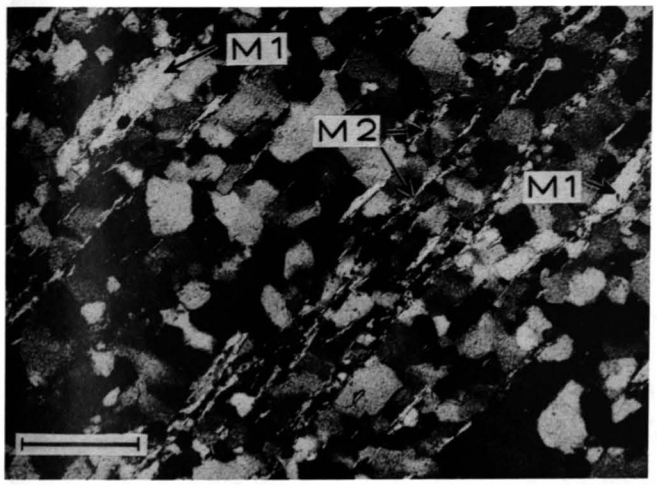

▲ a

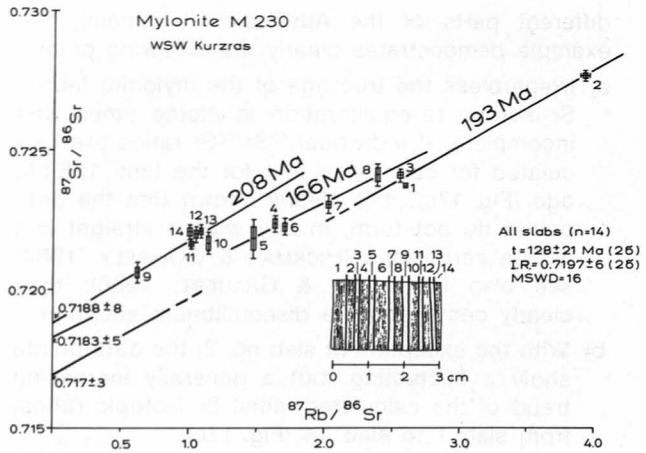

▲ b

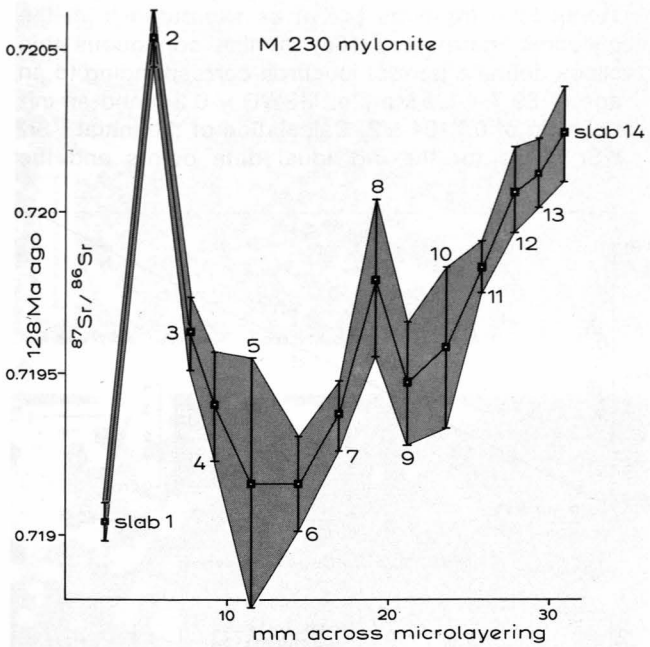

◀ c

Fig. 17.
a) Dynamically recrystallized microfabric of mylonite M230 (loc. 2 in Fig. 2), showing polygonal quartz, with some grains exhibiting strain-driven grain boundary migration, and tight preferred orientation of white mica.
Two strikingly different grain sizes of mica are observed: a coarser, probably pre-Alpine generation (partly fish-like, M_1) and a fine-grained one (M_2).
Sale bar = 0.3 mm.
b) Rb/Sr evolution diagram for 14 thin whole rock slices (microlayers) of mylonite M230.
The data distribution reflects a diffuse staircase pattern which is explained by preferred inhibition of Sr isotopic exchange at different levels, across microlayering. Regression ages shown are meaningless.
c) Plot of $^{87}Sr/^{86}Sr$ initial ratios vs. layer dimensions, for the time 128 Ma B.P. (which corresponds to the mean slope).
The continuous increase of the ratios from slab 4 to 14 may be interpreted by incomplete Alpine isochron rotation in a pre-Alpine system. Another explanation could be a varying but somehow systematic contamination of the system by infiltrating fluids, causing gradients in $^{87}Sr_{rad}$ concentration.

Table 2.
Rb-Sr data of mylonite M230 (WAP1383), WSW Kurzras.

Slab	ppm Rb	ppm Sr	$^{87}Rb/^{86}Sr$	$^{87}Sr/^{86}Sr \pm 2\sigma_m$
1	23.55	26.76	2.5876	0.72375± 6
2	28.86	19.94	3.9172	0.72766± 9
3	18.98	21.65	2.4584	0.72410±11
4	24.05	42.84	1.6320	0.72237±17
5	15.77	31.22	1.4694	0.72183±39
6	18.10	30.91	1.7027	0.72225±15
7	19.08	27.38	2.0261	0.72306±11
8	16.21	19.79	2.3806	0.72412±24
9	9.40	44.09	0.6197	0.72060±19
10	10.89	27.70	1.1429	0.72166±25
11	12.69	36.64	1.0065	0.72166± 8
12	12.40	34.41	1.0476	0.72197±13
13	12.85	34.52	1.0822	0.72209±11
14	9.44	27.52	0.9982	0.72206±15

mica is present as basically two well distinguishable grain sizes: a fine-grained one and a coarse one, both aligned perfectly parallel to the main foliation (equivalent to the macroscopically visible microlayering), and within an equant-grained, recrystallized quartz fabric (Fig. 17a). The relatively homogeneous fabric, the presence of only one, narrowly developed (probably S=C=shear) foliation and the generally symmetric shape of the coarse mica, interpreted as relictic fish-type clasts, all point to rather high shear strains (SIMPSON, 1984; cf. LISTER & SNOKE, 1984), but with high recrystallization rate/shear strain rate values (PASSCHIER & SIMPSON, 1986).

The Rb/Sr data points of 14 thin whole rock slices of this mylonite are plotted in Fig. 17b. As a whole, the data points exhibit considerable scatter (MSWD = 16), yielding a poorly defined regression age of 128 ±21 Ma (2σ) and an initial ratio of 0.7197 ±6. While this figure could be regarded to support in principle a post-Hercynian age for the mylonite (in fact, such Early Cretaceous ages are reported from

different parts of the Austroalpine domain), the example demonstrates clearly the following points.

a) Irregardless the true age of the mylonite fabric, Sr-isotope re-equilibration in Alpine times was incomplete. If individual $^{87}Sr/^{86}Sr$ ratios are calculated for each slice and for the time 128 Ma ago (Fig. 17c), it is clearly shown that the data points do not form, in any way, a straight line with a zero slope (HICKMAN & GLASSELY, 1984; see also BACHMANN & GRAUERT, 1986); they clearly demonstrate a disequilibrium situation.

b) With the exception of slab no. 2, the data points show a fluctuating, but a generally increasing trend of the calculated initial Sr isotopic ratios, from slab 1 to slab 14 (Fig. 17c).

c) This picture records some kind of systematic, but incomplete isochron rotation (partial resetting), by a post-Hercynian event; while this is the case for the sub-cm scale, more striking pre-existing isotopic heterogeneities were smoothed out only very incompletely on the cm-scale, as preserved e. g. by the isotopic pattern of layers 1–3 and 7–9 (Fig. 17c).

The fictive regression ages of between 208 and 166 Ma as shown in Fig. 17b could indicate similar, though still widely scattering, age loss in the different subvolumes of the example analyzed. If the mylonite fabric is interpreted as the product of intense Alpine deformation, incomplete isotopic resetting is explained by incomplete dynamic recrystallization, mainly within the coarse mica fishes, as well as irregular fluid flow, probably effective predominantly parallel rather than across the microlayering. Similar examples for the preservation of sharp discontinuities ("breaks" or "jumps") in small scale Sr isotopic profiles, and surviving partly amphibolite grade conditions, were earlier reported from the wider area of investigation (THÖNI, 1986).

3 A further example (T1521) is shown here only for comparison, mainly in order to further illustrate the general aspects as well as the success in dating shear zone rocks. It is a mylonite taken from a thrust zone, along which pre-Alpine basement has overridden weakly metamorphosed Permomesozoic rocks as described elsewhere in more detail (THÖNI, 1986). Fine fractions (<5 μ) as separated from the mylonitic matrix (Fig. 18a) of nine contiguous thin slices define a perfect isochron corresponding to an age of 89.7 ±1.4 Ma (2σ; MSWD = 0.24) and an initial ratio of 0.7194 ±2. Calculation of the initial $^{87}Sr/^{86}Sr$ ratios for the individual data points and the

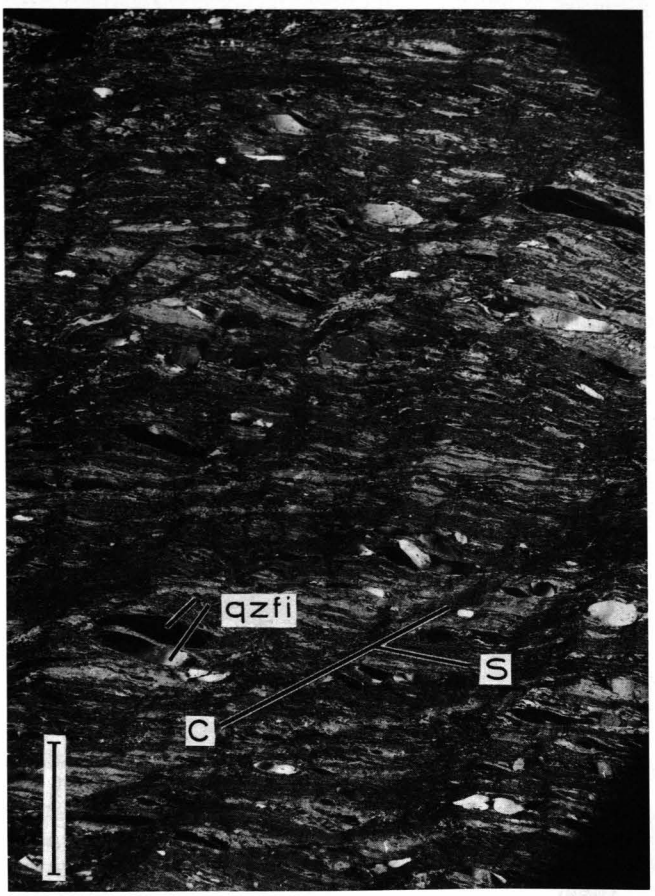

◀ a

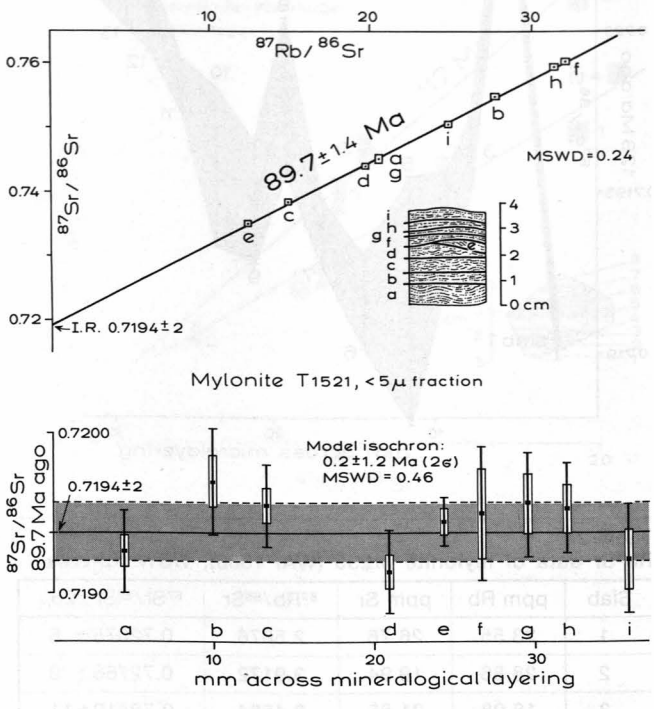

▲ b

Fig. 18.

a) Photomicrograph of mylonite T1521, loc. 3 in Fig. 2.
In this type of extensional crenulation cleavage microfabric (PLATT & VISSERS, 1980) stretched quartz fishes indicate a N to NW directed flow. Maximum extension (length/width ratios) of individual quartz grains (qzfi) reaches values of up to 20. Regional sense of tectonic movement is top-to-left in the example shown.
Scale bar = 5 mm.

b) Rb/Sr evolution diagram (top) and recalculated $^{87}Sr/^{86}Sr$ ratios (bottom) for the time indicated by the isochron, for nine fine fractions <5 μ of mylonite T1521. In this example, the very good fit of the data points as well as low variation of the initial $^{87}Sr/^{86}Sr$ ratios (which overlap within analytical errors; MSWD = 0.46) support the geologic significance of the age obtained. The 89.7±1.4 Ma (2σ) age is related to the mylonite formation.

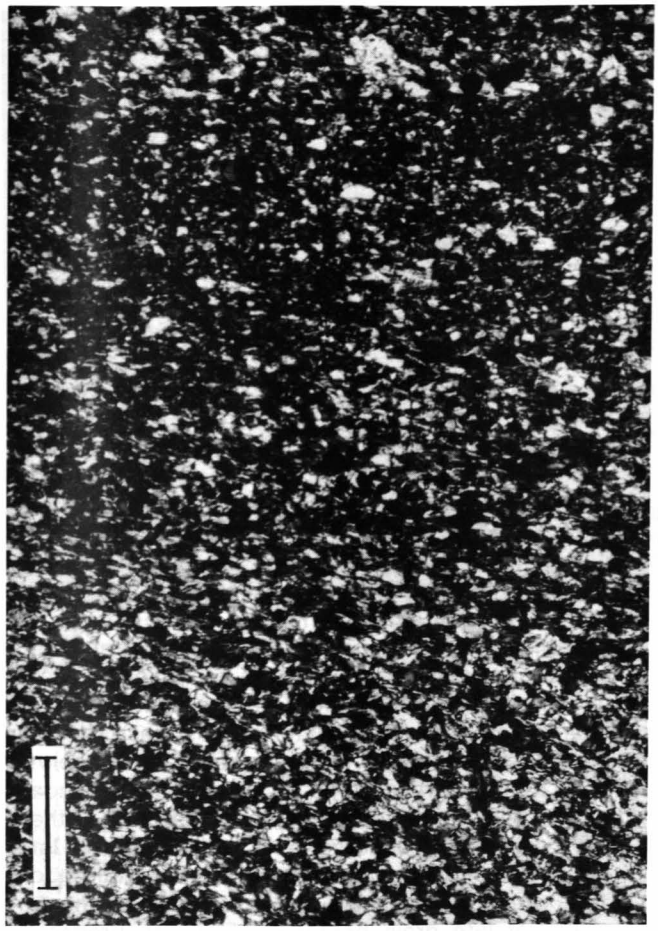

▲ a

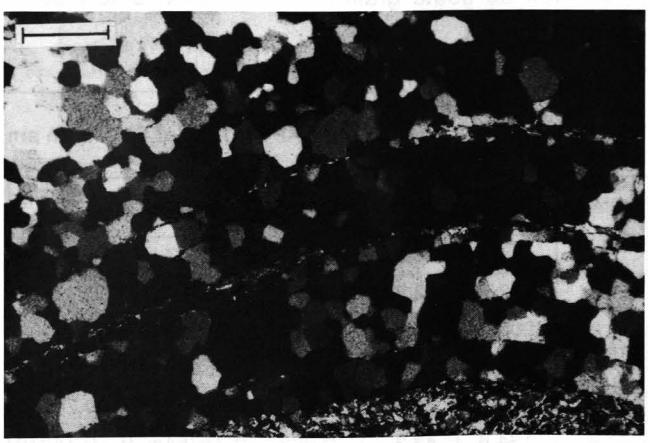

◀ b

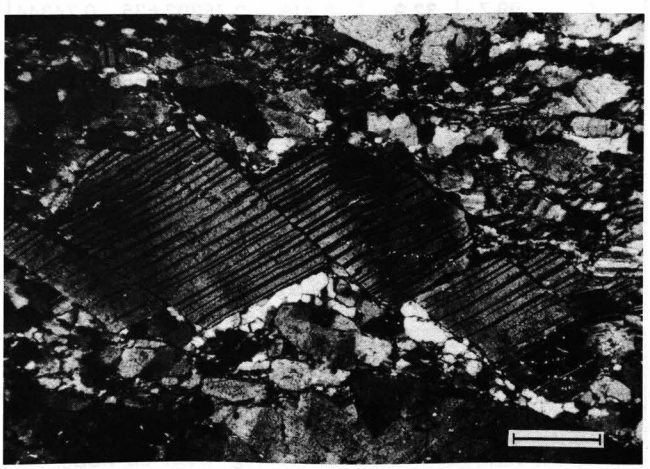

◀ c

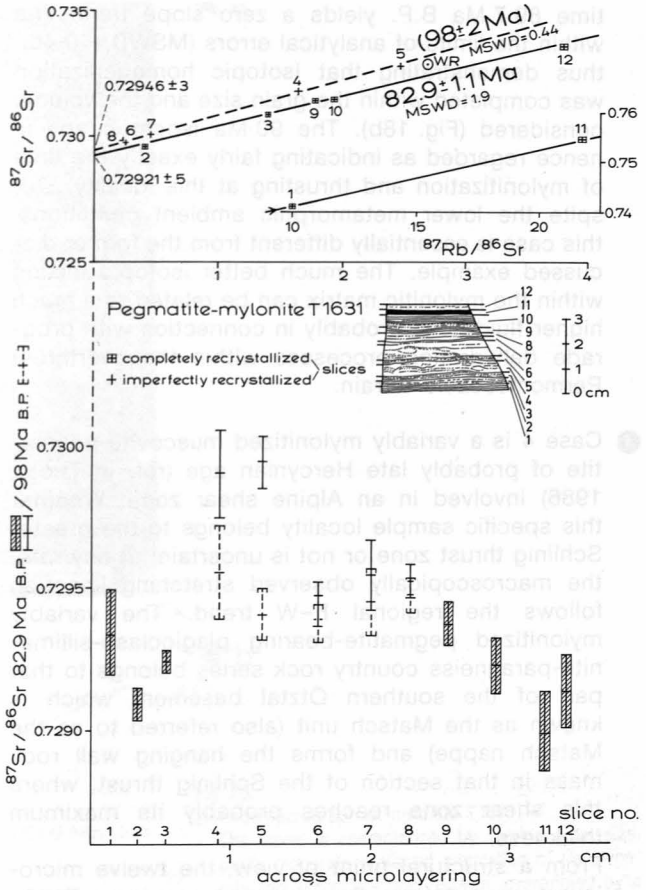

▲ d

Fig. 19.

a) Fine-grained, dynamically recrystallized, white mica-feldspar paragenesis (photomicrograph) from microlayers 10–11 of mylonite sample T1631. Regression of these two layers with a large spread in Rb/Sr yields an age of 82.1 Ma, which overlaps within the error limits with the age of the seven-point isochron as shown in Fig. 19d.
Scale bar = 0.2 mm.

b) Polygonal quartz recrystallization microstructure from microlayer 3 of the same mylonite sample T1631.
Along distinct narrow bands, defined by very fine-grained white mica, the polygonal shape of individual quartz grains is clearly truncated. This may point to grain growth inhibition, but more probably to rapid late deformation along distinct displacement zones, during quartz annealing.
Scale bar = 0.2 mm.

c) Bookshelf sliding (RAMSAY & HUBER, 1987) in a twinned broken plagioclase from the central, imperfectly recrystallized portion (microlayer no. 6) of sample T1631.
Scale bar = 0.2 mm.

d) Rb/Sr evolution for 12 contiguous microlayers of a pegmatite-mylonite with markedly varying dynamic recrystallization.
Whereas the 83±1 Ma regression age for the fine-grained layers 1–3 and 9–12 is interpreted as the true age of mylonitization, the 98±2 Ma figure for layers 4–8 is thought to be geologically meaningless. This latter portion of the specimen has preserved variable amounts of porphyroclast material (cf. Fig. 19c). Recalculation of the initial $^{87}Sr/^{86}Sr$ ratios (lower part of the graph) yields additional hints that the central portion of the specimen did not reach Sr isotopic re-equilibration during the 83 Ma mylonitization process.

time 89.7 Ma B.P. yields a zero slope trend line within the limits of analytical errors (MSWD = 0.46), thus demonstrating that isotopic homogenization was completed within the grain size and the volume considered (Fig. 18b). The 90 Ma isochron age is hence regarded as indicating fairly exactly the time of mylonitization and thrusting at this locality. Despite the lower metamorphic ambient conditions, this case is essentially different from the former discussed example. The much better isotopic mixing within the mylonitic matrix can be related to a much higher fluid flow, probably in connection with prograde dehydration processes within the overthrust Permomesozoic terrain.

❹ Case 4 is a variably mylonitized muscovite-pegmatite of probably late Hercynian age (ref. in THÖNI, 1986) involved in an Alpine shear zone. Whether this specific sample locality belongs to the greater Schlinig thrust zone or not is uncertain; at any rate, the macroscopically observed stretching lineation follows the regional E–W trend. The variably mylonitized pegmatite-bearing plagioclase-sillimanite-paragneiss country rock series belongs to that part of the southern Ötztal basement which is known as the Matsch unit (also referred to as the Matsch nappe) and forms the hanging wall rock mass in that section of the Schlinig thrust, where this shear zone reaches probably its maximum thickness.

From a structural point of view, the twelve microlayers as cut from the analyzed specimen T1631 (well distinguishable macroscopically by a variable colouring) may be grouped into three sections. Layers 1–3 an 9–12 are very similar and are characterized by a very fine and frequently equant grain size (Fig. 19a, b). They are interpreted to have undergone almost complete grain size reduction and dynamic recrystallization. In contrast, layers 4–8 are much coarser grained; they have preserved variable amounts of porphyroclast material (Fig. 19c).

Correspondingly, the data points for the twelve microlayers are arrayed along two tie lines with significantly different slopes and initial ratios. The regression ages obtained are 98 ±2 Ma (1σ) for those slices that preserved partly pre-mylonitic textures and 82.9 ±1.1 Ma for the two recrystallized sections. Different combinations of data points give age results between 81.9 and 84.8 Ma, with clearly overlapping 2σ error limits. If the MSWD values of the two regression lines as shown in Fig. 19d are compared, it is striking that the 98 Ma data points show a significant better fit (MSWD = 0.44) compared with MSWD = 1.9 of the rest. But obviously this age figure has no geological meaning. It is an artefact generated by the combined effect of thermal overprint and dynamic recrystallization during the 83 Ma mylonitization process (as recorded by the data points of the adjoining sections) and documents a surprisingly regular but still incomplete isochron rotation on the small scale. If the initial $^{87}Sr/^{86}Sr$ isotopic ratios are recalculated for the time 98 Ma B.P. (see lower part of Fig. 19d), the disequilibrium situation is fairly evident, however, demonstrating that within the microlayers 4–8 the Sr isotopes were not in mutual equilibrium 98 Ma ago.

Due to the large dispersion in Rb/Sr and also because of the very fine-grained mylonitic texture, which shows no evidence for "undigested" porphyroclast material, the best estimation for the mylonitization process in question is clearly derived from microlayers 10–12 (whereas slice 9, a transition layer between completely and incompletely recrystallized sections, seems to lie somewhat apart): they define an age of 82.1 ±0.5 Ma (1σ; I.R. = 0.72922 ±4; MSWD = 0.17). This date is related with distinct thrusting at falling eo-Alpine temperatures.

❺ One final example to be discussed briefly (T1571) comes from the eastern part of the Schlinig thrust where it has evolved into a ductile shear zone of considerable thickness. It is a strongly sheared two-mica-orthogneiss, collected near St. Martin am Kofel, some 4 km WSW of Texelspitze (Fig. 2). Eo-Alpine metamorphic temperatures are estimated as high as ≥500°C. The clearly developed microlayering (cm to mm scale) exhibits a rather coarse but variable grain size and moderate alignment of the constituent minerals (quartz, plagioclase, K-feldspar, white mica, light brown biotite, locally coarse patches of carbonate, accessories). No clear relict (= premylonitic) mineral phases are observed (Fig. 20a). Whereas some layers exhibit secondary grain growth and collective crystallization, others have obviously undergone a more intense later grain size reduction and dynamic recrystallization. The whole paragenesis, however, shows the imprints of late grain boundary migration processes as well as some grain-internal plastic deformation (quartz).

Table 3.
Rb-Sr data of mylonite T1571 (WAP1397), E of St. Martin am Kofel.

Slab	ppm Rb	ppm Sr	$^{87}Rb/^{86}Sr$	$^{87}Sr/^{86}Sr \pm 2\sigma_m$	$^{87}Sr/^{86}Sr$ 76.5 Ma ago
1	17.8	5.08	10.22	0.75697±20	0.74587
2	132.3	42.6	9.065	0.75484±10	0.74501
3	203.8	27.0	22.00	0.76829±11	0.74440
4	150.3	40.9	10.72	0.75528±11	0.74364
5	92.6	31.9	8.476	0.75366± 9	0.74445
6	134.6	43.3	9.058	0.75254± 9	0.74270
7	99.7	32.9	8.818	0.75302±35	0.74344
8	93.2	29.8	9.111	0.75254± 9	0.74265
9	159.7	11.0	42.63	0.78962±33	0.74332
10	75.3	9.95	22.09	0.76897±12	0.74498
11	115.6	31.2	10.82	0.75664± 8	0.74489
12	205.8	11.7	51.51	0.80205±11	0.74611
13	95.0	17.2	16.11	0.76142±21	0.74393
14	226.0	16.9	39.90	0.78479±17	0.74234
15	98.5	39.8	7.221	0.75396± 5	0.74612
16	258.4	7.87	96.80	0.84801±33	0.74289
17	68.9	28.5	7.035	0.75015±12	0.74251
WR (kg size)	130.1	29.2	13.00	0.75927±15	0.74515

WR = whole rock.

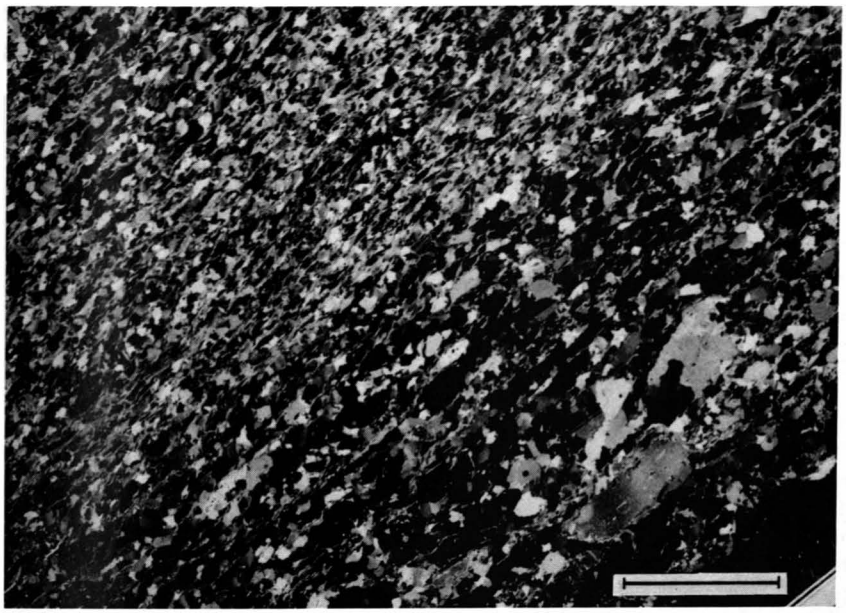

◀ a

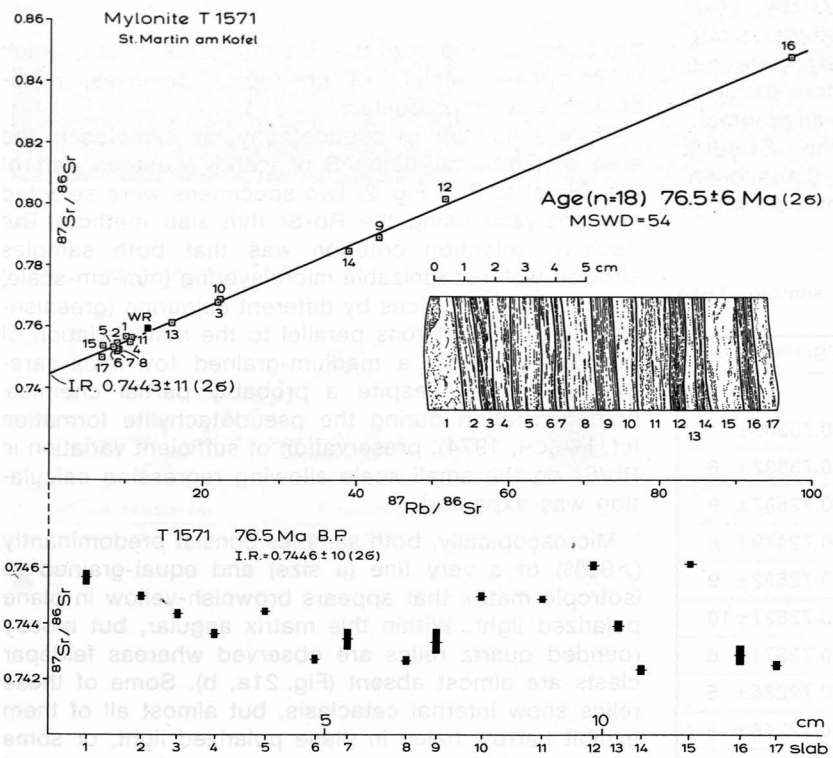

◀ b

Fig. 20.
a) Photomicrograph of mylonite T1571.
The fabric is characterized by varying grain size, partly moderate preferred orientation of the minerals and secondary grain growth, overprinted by a weak ongoing deformation (partly undulous extinction, serrated grain boundaries).
Scale bar = 2.5 mm.
b) Rb/Sr evolution diagram (top) and recalculated $^{87}Sr/^{86}Sr$ ratios (bottom; 76.5 Ma B.P.) for 17 thin slabs and the whole rock (WR) of mylonite T1571.
The data array is characterized by a strong scatter, but with regard to the high spread in Rb/Sr, icluding biotite-rich slabs, the regression age is thought to be basically meaningful. Note that the argument of lacking isotopic re-equilibration at the presumed time of mylonitization (76.5 Ma ago) is not valid, if a post-mylonitic perturbance of the system is taken into consideration.

The data points of 17 thin whole rock slabs (+WR) are plotted in Fig. 20b. As a whole, the data show exceptional scatter (MSWD= 54) along a trend line defining an age of 76.5 ±6 Ma (2σ) and an I.R. of 0.7443 ±11. Despite the poor fit, but in view of the large spread in Rb/Sr (7–97), this age figure is regarded as being basically significant, dating a penetrative mylonitization event close to 80 Ma. As no relict domains are recognized in thin section, the whole paragenesis seems to have dynamically recrystallized, and a better fit of the data points could be expected. In accordance with the microstructure observed, the scatter of the data points is best explained by some late to post-mylonitic effects, such as local grain boundary migration and recrystallization due to weak ongoing deformation, variable thermal imprints or closing conditions on the small (grain) scale (biotite, muscovite, feldspar), or even to a late fluid or metasomatic activity (carbonatization). As the slabs with high Rb/Sr ratios all contain biotite, the true age of mylonitization is most probably somewhat older, rather than younger, than the date given by the regression line. So far, this is one of the youngest age values found along the Schlinig thrust. In connection with the structures and microfabrics (Fig. 14) described, these data support intense shear deformation and west- to northwestward intra-Austroalpine thrusting at falling eo-Alpine temperatures.

8. Late Cretaceous Pseudotachylites in the Silvretta

Pseudotachylites have been known from many parts of the earth and from different geological settings (PHILPOTTS, 1964). Commonly, they are found along displacement zones and their generation is probably related to melting by frictional heating. Fusion is interpreted to originate from fast slip along distinct narrow zones, e.g. during faulting or landsliding (SHAND, 1916; GROCOTT, 1981; MASCH et al., 1985; see also SPRAY, 1987). Catastrophic events like earthquakes are seen as another possibility to produce pseudotachylites (SIBSON, 1975). Though the question concerning the physical and rheological state of the material at the time of formation (and emplacement) of a pseudotachylite is still being debated (e.g. WENK, 1978), it is clear that at least some examples described in the literature are products of fusion. This point is also of some importance for the present considerations.

In the western Austroalpine basement nappes pseudotachylites occur in different areas; some of them were discovered only recently (NW Ötztal, Texel area, etc.; Fig. 2). The most famous and extensive outcrops are known from the Silvretta. They were described by BEARTH (1933) and studied in more detail by MASCH (1974). However, age and tectonic environmental situation for the formation of the Silvretta pseudotachylites is still controversial (LAUBSCHER, 1983, for review). These rocks are concentrated within the basal ca. 300 m of the Silvretta thrust mass, which is composed mainly of pre-Alpine gneisses, micaschists and amphibolites.

Table 4.
Rb-Sr analytical data of pseudotachylite sample T644 (WAP617), Fimbertal/Silvretta basement.

Sample	ppm Rb	ppm Sr	$^{87}Rb/^{86}Sr$	$^{87}Sr/^{86}Sr \pm 2\sigma_m$
Thin slabs				
1	258.0	52.1	14.424	0.73309± 4
1*	267.0	48.2	16.138	0.73532± 6
2	211.5	75.2	8.182	0.72597± 9
3	201.1	98.8	5.921	0.72479± 6
4	220.9	81.7	7.860	0.72652± 9
5	249.6	71.2	10.200	0.72827±10
5*	252.9	76.2	9.660	0.72871± 6
6	191.0	145.8	3.810	0.72235± 5
6*	213.6	155.6	3.991	0.72246± 9
6*–7*	235.9	131.6	5.216	0.72394± 5
7	267.9	103.6	7.521	0.72583± 6
8	230.4	177.4	3.776	0.72389± 5
Fine fractions (FF) (from ca. 1 ccm sample volume; lateral extension of slabs 3–4)				
<5 μ	196.3	90.8	6.286	0.72526± 8
5–11μ	198.5	93.6	6.165	0.72526± 7
11–20μ	196.1	94.8	6.016	0.72521± 8
20–35μ	197.4	96.3	5.962	0.72539±19
35–63μ	201.6	97.9	5.986	0.72523±10
>63μ	207.1	100.4	5.994	0.72513±10
WR (0.15–0.25)*	225.8	92.7	7.086	0.72606± 4

*) Sieve fraction of crushed fist-size sample as used for K-Ar analysis. WR = whole rock.

Table 5.
Rb-Sr analytical data of pseudotachylite sample T645 (WAP618), Fimbertal/Silvretta basement.

Slab	ppm Rb	ppm Sr	$^{87}Rb/^{86}Sr$	$^{87}Sr/^{86}Sr \pm 2\sigma_m$	$^{87}Sr/^{86}Sr$ 78.5 Ma ago
1A	190.3	103.7	5.336	0.72452±19	0.71857
1B	188.1	97.0	5.640	0.72510± 8	0.71881
1C	184.2	103.2	5.190	0.72437± 9	0.71858
2	206.4	85.8	6.997	0.72645± 7	0.71865
3	201.0	78.9	7.416	0.72654±29	0.71827
4	212.4	62.9	9.842	0.72959±10	0.71862
5	178.7	127.1	4.086	0.72303± 8	0.71847
6	182.2	149.2	3.550	0.72244± 7	0.71848
7	169.7	119.8	4.120	0.72344± 6	0.71885
8	200.6	89.5	6.521	0.72925±12	0.72198
WR (0.15–0.25)*	201.7	94.1	6.231	0.72520±14	0.71825

*) Sieve fraction of crushed fist-size sample as used for K-Ar analysis. WR = whole rock.

From a number of pseudotachylites sampled in the area of Fimbertal/Idalpe S of Ischgl (Austrian part of the Silvretta; P in Fig. 2) two specimens were selected and analyzed using the Rb-Sr thin slab method. The decisive selection criterion was that both samples showed well recognizable microlayering (mm-cm-scale) on smoothly cut slices by different colouring (greenish-grey to pink) that runs parallel to the main foliation of the country rock, a medium-grained tow-mica-paragneiss. Hence, despite a probably partial chemical homogenization during the pseudotachylite formation (cf. MASCH, 1974), preservation of sufficient variation in Rb/Sr on the small scale allowing regression calculation was expected.

Microscopically, both samples consist predominantly (>90%) of a very fine (μ size) and equal-grained to isotropic matrix that appears brownish-yellow in plane polarized light. Within this matrix angular, but mostly rounded quartz relics are observed whereas feldspar clasts are almost absent (Fig. 21a, b). Some of these relics show internal cataclasis, but almost all of them exhibit narrow halos in plane polarized light, or some kind of resorption phenomena, that can be interpreted as reaction rims formed during a melting process. From X-ray analyzes that show poorly developed reflexes for quartz, and subordinately albite and mica it may be deduced that the homogeneous matrix represents poorly recrystallized glass. Contacts to the unaltered biotite-plagioclase-gneiss are sharp and in one case schlieren-like flow structures were observed. In addition, sample T644 shows later, discordant veins of (sub-)mm size, filled with chlorite, quartz and carbonate (as indicated on slabs 2 and 5 of Fig. 21c). Along these gashes, the fine-grained pseudotachylite matrix is intensely bleached over some 100 μ.

The Rb-Sr thin slab results for the two analyzed samples T644 and T645 are listed on Tabs. 4 and 5, the plots in Fig. 21c, d show moderate scatter of the data points along the calculated regression lines (MSWD = 5.24 and 2.26); the resulting age values are

73 ±3.2 Ma for T644 (n = 9) and 78.5 ±4.6 Ma (n = 9; 2σ) for T645. Data points shown in paranthesis are not included in the regression calculation. In both cases, the data point for the nearly unaltered paragneiss wall rock (slabs no. 8) plot clearly off the corresponding tie line. Slabs 2 and 5 of sample T644 plot below the regression line for the remaining points; they obviously suffered ^{87}Sr loss during the later vein filling event.

▲ a

▲ b

Fig. 21.
a, b) Photomicrographs of pseudotachylite sample T644.
Within a very fine grained homogeneous matrix "undigested" and varyingly rounded quartz relics are recognized. Microlayering on the mm scale, as observed in some sections of sample T644 is interpreted as relict structure of the paragneiss, rather than as fluxion structure. Additionally, a late chlorite vein (chl) can be observed in the upper left.
Scale bar = 0.15 mm for both a and b.

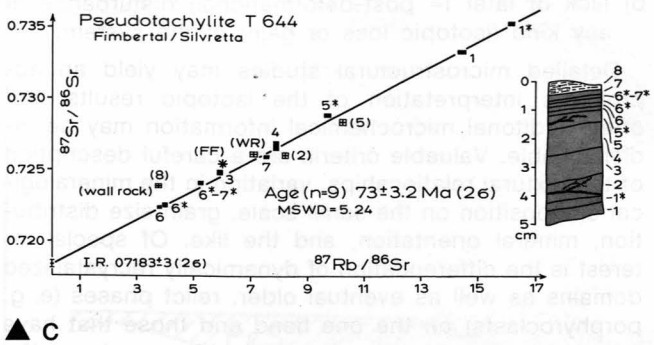

▲ c

c) Rb/Sr evolution diagram for thin slabs, different fine fractions (FF) and the whole rock of pseudotachylite sample T644.
Samples in paranthesis are not included in the regression calculation. Slabs 2 and 5 are omitted because of the secondary alteration of the material along later veins.

d) Rb/Sr evolution diagram (top) and recalculated $^{87}Sr/^{86}Sr$ ratios (below) for the time 78.5 Ma B.P. for pseudotachylite T645.
The regression age overlaps within the error limits with the one of the former example and the recalculated $^{87}Sr/^{86}Sr$ ratios exhibit moderate scatter along a 0 Ma trendline, thus supporting fairly perfect isotopic homogenization within the volume analyzed at the time as defined. Both data sets (T644, T645) are related to the main pseudotachylite forming event.

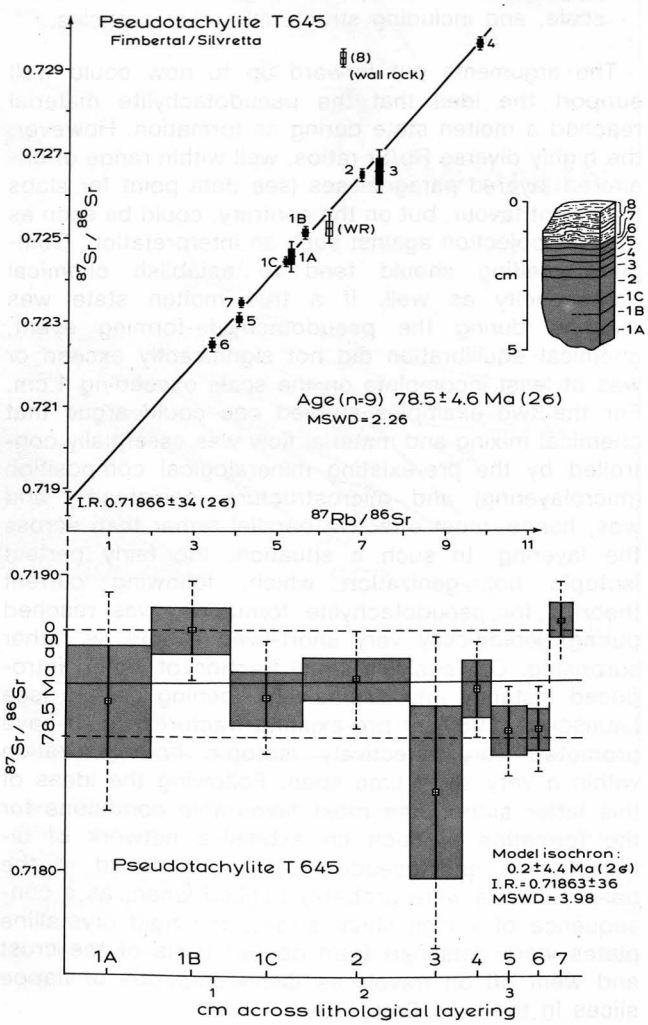

d ▶

Polyphase evolution of the Silvretta pseudotachylites was already recognized by BEARTH (1933).

Earlier K-Ar studies on whole rock fractions of seven pseudotachylite samples from the Fimbertal/Idalpe area, including the two samples here described, yielded model ages between 53 to 58 Ma, 73 to 78 Ma and 114 Ma (THÖNI, 1981). Different interpretations for these data were discussed, but a Late Cretaceous age for the main pseudotachylite formation event was preferred.

The two regression ages reported here are interpreted as reflecting the time of pseudotachylite formation. This means that fairly perfect homogenization of the Sr isotopes was achieved by a very short-lived shock event in "dry" basement rocks some 75 Ma ago. Two additional informations support this interpretation.

a) Calculation of the inital $^{87}Sr/^{86}Sr$ ratios for the individual slabs of sample T645 shows linear array within analytical errors and with a 0 Ma slope. This points to complete resetting as well as pervasive isotopic homogenization in the whole rock over some 3 cm (Fig. 21d).
b) From sample T644, six different grain size fractions (as produced artificially by short grinding and sedimentation) were analyzed from a ca. 1 ccm rock volume. From the finest to the coarsest fraction (FF, Fig. 21c and Tab. 4), the $^{87}Sr/^{86}Sr$ and $^{87}Rb/^{86}Sr$ ratios are identical within analytical errors, thus supporting perfect isotopic homogenization on the cm scale, and including structurally relict particles.

The arguments put forward up to now could well support the idea that the pseudotachylite material reached a molten state during its formation. However, the highly diverse Rb/Sr ratios, well within range of unaltered layered paragneisses (see data point for slabs 8), do not favour, but on the contrary, could be seen as a major objection against such an interpretation. Complete melting should tend to establish chemical homogeneity as well. If a true molten state was reached during the pseudotachylite-forming event, chemical equilibration did not significantly exceed or was at least incomplete on the scale exceeding 1 cm. For the two examples studied one could argue that chemical mixing and material flow was essentially controlled by the pre-existing mineralogical composition (microlayering) and microstructure (schistosity) and was, hence, most effective parallel rather than across the layering. In such a situation, the fairly perfect isotopic homogenization which, following current theories for pseudotachylite formation, was reached during geologically very short-lived events, is rather surprising. Obviously, a small fraction of water, introduced instantly into explosively opening gashes (see LAUBSCHER, 1983) or pre-existing fractures could have promoted very effectively isotopic homogenization within a very short time span. Following the ideas of this latter author, the most favourable conditions for the formation of such an extensive network of ultramylonites and pseudotachylites as found in the basal Silvretta were probably fulfilled when, as a consequence of a high shear stress, the rigid crystalline plates were detached from deeper parts of the crust and went off on travels as distinct nappes or nappe slices in the Late Cretaceous.

9. Discussion

For mylonites s.str. (WISE et al., 1984), the Rb/Sr thin slab (or small scale) method of dating may provide essential information on the timing of deformation as well as the scale of isotopic resetting. In addition, this method has the advantage, that

a) no time-consuming mineral separation is required, which is often very difficult in fine-grained rocks and
b) all the minerals involved in the deformation process are considered.

For rocks undergoing pervasive deformation at low-grade conditions, application of the closing temperate model is inappropriate: all the constituent minerals are interpreted to record the end of a dynamic (re)crystallization process rather than stepwise closing; hence the age as gained for a small whole rock specimen should reflect the mean time of isotopic resetting for the different minerals of the paragenesis under consideration.

However, such ideal cases are rarely fulfilled in nature, especially in polyphase metamorphic rocks. Geological interpretation of such deformation ages may often be a rather difficult attempt. It is, in the first place, dependent on the microstructural intepretation which includes the estimation of two basic preconditions for a strict time significance of isotopic ages, namely

a) complete resetting (isotopic homogenization) within the volume considered during the event to be dated and
b) lack of later (= post-deformational) disturbance of any kind (isotopic loss or gain) of the system.

Detailed microstructural studies may yield an appropriate interpretation of the isotopic results, but often additonal microchemical information may be indispensable. Valuable criteria are a careful description of the textural relationships, variation in the mineralogical composition on the samll scale, grain size distribution, mineral orientation, and the like. Of special interest is the differentiation of dynamically recrystallized domains as well as eventual older, relict phases (e. g. porphyroclasts) on the one hand and those that have been altered by some post-mylonitic event on the other. For most of the samples discussed in this paper it is possible to explain the position or deviation of a specific data point in the Rb/Sr evolution diagram by petrographic observations. In such cases where a fine-grained mylonitic matrix and coarse-grained relictic porphyroclast material are recognized, separation of the neogenic material requires very careful techniques. Nonetheless, it has been shown that this method of dating neogenic fine fractions from contiguous thin layers in mylonites is in some cases also successful.

One possibility to test the scale and extent of isotopic homogenization is to calculate the "initial" $^{87}Sr/^{86}Sr$ isotopic ratios for the individual data point of a coherent sample (e.g. slab suite), for the time B.P. as defined by the relative tie line (see HICKMAN & GLASSLEY, 1984). If no marked isotopic inhomogeneities are recorded and the sample suite defines a zero slope age within analytical errors, then complete isotopic resetting during the last deformation event is probable and the regression age may be regarded as a geologically meaningful figure. Good examples for this are shown in Figs. 18b, 19d and 21d. The technique, however, cannot distinguish between inherent isotopic in-

homogeneities (not smoothed out during the deformation event of interest) and later, post-mylonitic disturbance. Hence, its application is limited, and badly scattering regression lines (errochrons, like the one shown e.g. in Fig. 20b) can not be "tested" in this respect.

A severe limitation for the application of the thin slab method is the rather frequent occurrence of sudden isotopic jumps or breaks in coherent sample suites, that do, all the more, occur often without mineralogical or structural inhomgeneities. Intense shearing combined with a syn-deformational fluid flow preferably parallel to a pre-existing microlayering may partly smooth out such breaks, but to a variable extent. In such cases, the resulting Rb-Sr pattern is a gently staircase one, giving rise to subparallel tie lines, if the degree of isotopic resetting is similar throughout the volume observed. The example shown in Figs. 17b, c, illustrates some aspects of such a complex system. Introduction of Sr of extraneous isotopic composition via a fluid phase during the mylonitization may further complicate the situation.

Regardless of these limitations, however, Rb-Sr analysis of thin whole rock slices of ultramylonites and mylonites (or, alternatively, of fine fractions separated therefrom) may provide an essentially powerful geochronological tool, able to answer questions that are not resolvable using other analytical methods.

10. Geologic implications

Considering the data presented in this paper within a regional geologic frame, and in order to test their significance with respect to the timing of nappe detachment, transport and emplacement as well as nappe-internal deformation, some of the following facts are useful to be remembered (cf. Fig. 2).

- According to paleontological evidence the youngest marine sediments are of Aptian to max. M-Turonian age in the Ortler nappe (CARON et al., 1982) and Aptian–Albian to possibly Cenomanian in the northeastern Engadine Dolomites (MADER, 1983). These latter

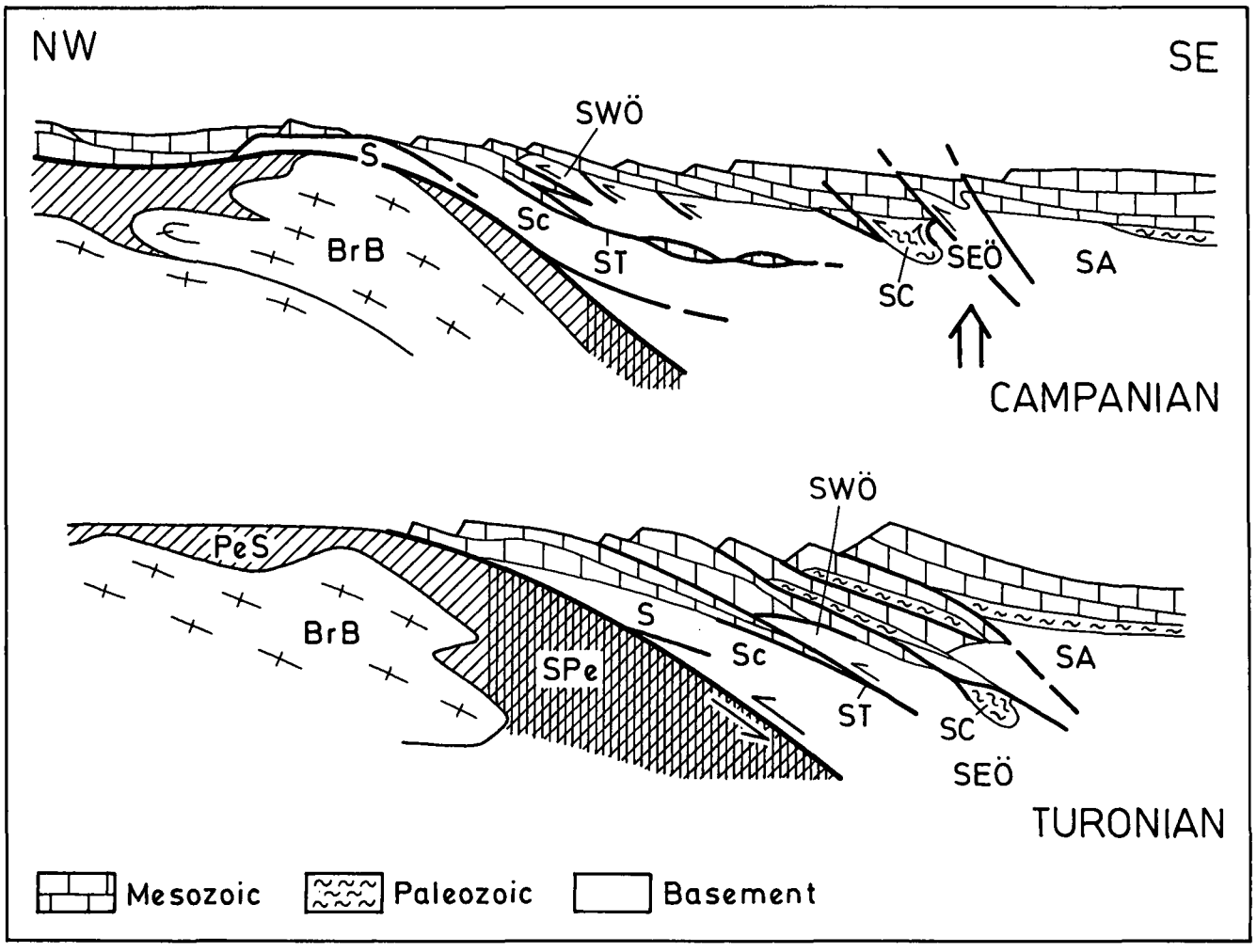

Fig. 22.
Tentative reconstruction of two successive evolution steps of the Austroalpine nappes under consideration for the Late Cretaceous.
The lower part of the figure illustrates the stage of decompression (corresponding to the climax of the last metamorphic recrystallization) and beginning exhumation, following a phase of burial (at variable depths and for an unknown period of time).
The upper part of the figure shows, that uplift, tectonic dismembrement and thrusting at different levels has finally interrupted the eo-Alpine metamorphism within the Austroalpine domain. This initiation of detachment, as reflected by the different deformation and cooling ages, may have its primary cause in the final collision of the Briançonian with the Adriatic microplate.
BrB = Briançonia Basement; PeS = Pennine sediments; SPe = South Pennine "trough"; S = Silvretta; Sc = Scarl unit; ST = Schlinig thrust zone; SC = Schneeberg complex; SWÖ = southwestern Ötztal basement; SEÖ = southeastern Ötztal basement; SA = Southalpine units.
Scale is not proportional.

data set an important upper age limit for the Schlinig thrust.

- The actual emplacement of the Silvretta is of post-Middle Eocene age, following the new finds by RUDOLPH (1982), OBERHAUSER (1983) and earlier investigations by TORRICELLI (1956).
- Radiometric and petrographic-sedimentological data by DEUTSCH (1983) and possibly also those of WINKLER & BERNOULLI (1986) place additional constraints on the pT-situation of subducted Pennine areas. DEUTSCH (1983) postulates "an eoalpine event already in Aptian-Albian times" for the Penninic Platta nappe (an area immediately adjoining the southwestern Silvretta basement; labelled "A" in Fig. 2b) on the basis of K-Ar data on syn- to postkinematically crystallized blue amphiboles. WINKLER & BERNOULLI (1986), on the other hand, described detrital high-P/low-T metamorphic minerals (lawsonite and glaucophane) from a Turonian flysch sequence of the Pennine-Austroalpine transition zone (labelled "B" in Fig. 2a). A very rapid exhumation is postulated by the authors for these high-p components, if they were formed during the eo-Alpine subduction-collision event. It is therefore important to emphasize here, that both these data concern a time when metamorphism was still going on in the Austroalpine units.

A review of the available Alpine metamorphic ages from the Austroalpine units under consideration (Fig. 11) clearly shows that regional cooling set on in the time interval between 90 (Turonian) and 80 Ma (L. Campanian).

If the interruption of the thermal metamorphism within the Austroalpine nappes is seen in causal connection with the rapid underplating by a northern European continent, and as a consequence, final décollement and cooling within the crust above, a process that is frequently placed in Mid- to Late Cretaceous time (e.g. FRISCH, 1981; OXBURGH & ENGLAND, 1980; cf. PLATT, 1986), then paleontological-sedimentological and radiometric evidence still seem to be in line with each other. It should be emphasized, however, because of partial contemporaneity of radiometric data and paleontological evidence, that the overall tectonometamorphic evolution must have been fairly rapid at this time (cf. DAL PIAZ et al., 1972; see Fig. 22). Rather undisturbed sedimentation was partly still continuing in higher tectonic levels and at the same time, metamorphism and deformation processes governed deeper parts of the crust. Furthermore it is evident from Fig. 11, that most of the deformation ages as gained from mylonitic rocks coincide with the process of regional cooling. If an important collision event took place in the early Late Cretaceous, the mylonite ages could mark the time of a special stress situation in the underplated Austroalpine crust, and, more exactly, internal small- and large-scale disruption and final offshearing and going off on travels of the Austroalpine nappes.

Acknowledgements

Field and laboratory work was supported by the Fonds zur Förderung der wissenschaftlichen Forschung, Wien. Form and content of the present paper were substantially improved by comments of G. EISBACHER (Karlsruhe), L. RATSCHBACHER (Tübingen), J. L. PAQUETTE (Rennes, Zürich) and J. C. HUNZIKER (Bern). Special thanks are due to CHRISTIAN HOHENEGGER, owner of Weißkugelhütte, for providing invaluable support during field work. I thank MONIKA JELENC for the untiring technical assistence, L. LEITNER for brilliantly drafting the figures, A. HAMMERMÜLLER and K. KARISCH for preparing several dozens of excellent thin sections, R. GOLD for the outstanding photographic work and last but not least my wife MONIKA for typing and retyping the manuscript.

References

AFTALION, M. & VAN BREEMEN, O.: U-Pb Zircon, Monazite and Rb-Sr Whole Rock Systematics of Granitic Gneiss and Psammitic to Semi-Pelitic Host Gneiss from Glenfinnan, Northwestern Scotland. – Contrib. Mineral. Petrol., **72**, 87–98, Heidelberg 1980.

ASHKINADZE, G. Sh., GOROKHOVSKIY, B. M. & SHUKOLYUKOV, Yu. A.: $^{40}Ar/^{39}Ar$ Dating of Biotite Containing Excess $^{40}Ar^{*}$. – Geochem. Internat., **14**/3, 172–176, Washington 1977.

BACHMANN G. & GRAUERT, B.: Dating by means of $^{87}Sr/^{86}Sr$-Disequilibrium Profiles. – Terra cognita, **6**, 148, Cambridge 1986.

BEARTH, P.: Über Gangmylonite der Silvretta. – Schweiz. mineral. petrogr. Mitt., **13**/2, 347–355, Zürich 1933.

BEHRMANN, J. H.: A precautionary note on shear bands as kinematic indicators. – J. Struct. Geol., **9**/5–6, 659–666, Oxford 1987.

BERTHÉ, D., CHOUKROUNE, P. & JEGOUZO, P.: Orthogneiss, mylonite and non coaxial deformation of granites: the example of the South Armorican Shear Zone. – J. Struct. Geol., **1**, 31–42, Oxford 1979.

BUHL, D. & GRAUERT, B.: Untersuchungen zur Strontium-Diffusion im Übergangsbereich Amphibolit-/Granulitfazies. – Fortschr. Mineral., **63**, Beih. 1, 276, Stuttgart 1985.

CARON, M., DÖSSEGGER, R., STEIGER, R. & TRÜMPY, R.: Das Alter der jüngsten Sedimente der Ortler-Decke (Oberostalpin) in der Val Trupchun (Schweizerischer Nationalpark, Graubünden). – Eclogae geol. Helv., **75**/1, 159–169, Basel 1982.

CHAMBERLAIN, C. P. & KARABINOS, P.: Influence of deformation on pressure-temperature paths of metamorphism. – Geology, **15**, 42–44, Boulder/Col. 1987.

CHOPIN, Ch. & MALUSKI, H.: ^{40}Ar–^{39}Ar Dating of High Pressure Metamorphic Micas From the Gran Paradiso Area (Western Alps): Evidence Against the Blocking Temperature Concept. – Contrib. Mineral. Petrol., **74**, 109–122, Heidelberg 1980.

CLAR, E.: Review of the Structure of the Eastern Alps. – In: JONG, K. DE & SCHLOTEN, E. (Eds.): Gravity & Tectonics, 253–270, New York (Wiley) 1973.

CLIFF, R. A.: Isotopic dating in metamorphic belts. – J. Geol. Soc. London, **142**, 97–110, London 1985.

DAL PIAZ, G. V. & ERNST, W. G.: Areal geology and petrology of eclogites and associated metabasites of the Piemonte ophiolite nappe, Breul – St. Jaques area, Italian Western Alps. – Tectonophysics, **51**, 99–126, Amsterdam 1978.

DAL PIAZ, G. V., HUNZIKER, J. C. & MARTINOTTI, G.: La zona Sesia-Lanzo e l'evoluzione tettonico-metamorfica delle Alpi nordoccidentali interne. – Mem. Soc. Geol. It., **11**, 433–460, Pisa 1972.

DEL MORO, A., PUXEDDU, M., RADICATI DI BRONZOLO, F. & VILLA, I. M.: Rb-Sr And K-Ar ages on minerals at temperatures of 300–400°C from deep wells in the Larderello Geothermal Field (Italy). – Contrib. Mineral. Petrol., **81**, 340–349, Heidelberg 1982.

DEL MORO, A., SASSI, F. P. & ZIRPOLI, G.: New radiometric data on the Alpine thermal history in the Oetztal – Merano area (Eastern Alps). – Mem. Sci. Geol., **35**, 319–325, Padova 1982.

DESMONS, J., HUNZIKER, J. C. & DELALOYE, M.: Unconvincing Evidence Against the Blocking Temperature Concept. – Contrib. Mineral. Petrol., **80**, 386–390, Heidelberg 1982.

DEUTSCH, A.: Datierungen an Alkaliamphibolen und Stilpnomelan aus der südlichen Platta-Decke (Graubünden). – Eclogae geol. Helv., **76**/2, 295–308, Basel 1983.

DEUTSCH, A. & STEIGER, R. H.: Hornblende K-Ar ages and the climax of Tertiary metamrophism in the Lepontine Alps (south-central Switzerland): an old problem reassessed. – Earth and Plan. Sci. Lett., **72**, 175–189, Amsterdam 1985.

DODSON, M. H.: Closure Temperature in Cooling Geochronological and Petrological Systems. – Contrib. Mineral. Petrol., **40**, 259–274, Heidelberg 1973.

DODSON, M. H.: Kinetic processes and thermal history of slowly cooling solids. – Nature, **259**, 551–553, London 1976.

ETHERIDGE, M. A., WALL, V. J. & VERNON, R. H.: The role of the fluid phase during regional metamorphism and deformation. – J. metamorphic Geol., **1**, 205–226, Oxford 1983.

FLISCH, M.: Die Hebungsgeschichte der oberostalpinen Silvretta-Decke seit der mittleren Kreide. – Bull. Ver. Schweiz. Petroleum-Geol. u. -Ing., **53**/123, 23–49, Basel 1986.

FOLAND, K. A.: $^{40}Ar/^{39}Ar$ incremental heating plateaus for biotites with excess argon. – Isotope Geosci., **1**, 3–21, Amsterdam 1983.

FRANK, W.: Evolution of the Austroalpine Elements in the Cretaceous. – In: H. W. FLÜGEL & P. FAUPL (Eds.): Geodynamics of the Eastern Alps, 379–406, Wien (Deuticke) 1987.

FREER, R.: Diffusion in Silicate Minerals and Glasses: A Data Digest and Guide to the Literature. – Contrib. Mineral. Petrol., **76**, 440–454, Heidelberg 1981.

FRISCH, W.: Plate motions in the Alpine region and their correlation to the opening of the Atlantic ocean. – Geol. Rundschau, **70**, 402–411, Stuttgart 1981.

FRIZZO, P. & CARNALE, P.: Geologia e metallogenesi nell'area di San Martino di Monteneve/Schneeberg – Val Lazzago (Alto Adige). – Boll. Soc. Geol. It., **100**, 467–487, Roma 1981.

FYFE, W. S.: Chemical aspects of rock deformation. – Phil. Trans. R. Soc. London, **A.283**, 221–228, London 1976.

GOOL, J. A. M. VAN, KEMME, M. M. J. & SCHREURS, G. M. M.F.: Structural Investigations along an E-W Cross-Section in the Southern Ötztal Alps. – In: H. W. FLÜGEL & P. FAUPL (Eds.), Geodynamics of the Eastern Alps, 214–225, Wien (Deuticke) 1987.

GRAUERT, B.: Die Entwicklungsgeschichte des Silvretta-Kristallins auf Grund radiometrischer Altersbestimmung. – Inauguraldiss. Univ. Bern, 166 S., München (Photodruck) 1969.

GRIFFIN, W. L. & BRUECKNER, H. K.: REE, Rb-Sr and Sm-Nd studies of Norwegian eclogites. – Chem. Geol. (Isotope Geosci. Sect.), **52**, 249–251, Amsterdam 1985.

GROCOTT, J.: Fracture geometry of pseudotachylyte generation zones: a study of shear fractures formed during seismic events. – J. Struct. Geol., **3**/2, 169–178, Oxford 1981.

HARRISON, T. M.: Diffusion of ^{40}Ar in Hornblende. – Contrib. Mineral. Petrol., **78**, 324–331, Heidelberg 1981.

HARRISON, T. M., ARMSTRONG, R. L., NAESER, C. W. & HARAKAL, J. E.: Geochronology and thermal history of the Coast Plutonic complex, near Prince Rupert, British Columbia. – Canadian Jour. Earth Sci., **16**, 400–410, Ottawa 1979.

HART, S. R.: The Petrology and Isotopic-Mineral Age Relations of a Contact Zone in the Front Range, Colorado. – Jour. Geol., **72**, 493–525, Chicago 1964.

HICKMAN, M. H. & GLASSLEY, W. E.: The role of metamorphic fluid transport in the Rb-Sr isotopic resetting of shear zones: evidence from Nordre Strømfjord, West Greenland. – Contrib. Mineral. Petrol., **87**, 265–281, Heidelberg 1984.

HOFMANN, A. W.: Diffusion Experiments in Isotope Geology. – In: E. JÄGER & J. C. HUNZIKER (Eds.): Lectures in Isotope Geology, 189–193, Berlin – Heidelberg (Springer) 1979.

HOFMANN, A. W. & HART, S. R.: An assessment of local and regional isotopic equilibrium in the mantle. – Earth Plan. Sci. Lett., **38**, 44–62, Amsterdam 1978.

HOINKES, G.: Mineralreaktionen und Metamorphosebedingungen in Metapeliten des westlichen Schneebergerzuges und des angrenzenden Altkristallins (Ötztaler Alpen). – Tschermaks min. petr. Mitt., **28**, 31–54, Wien 1981.

HOINKES, G., FRANK, W., MAURACHER, J., PESCHEL, R., PURTSCHELLER, F. & TESSADRI, R.: Petrography of the Schneeberg Complex. – In: H. W. FLÜGEL & P. FAUPL (Eds.): Geodynamics of the Eastern Alps, 190–199, Wien (Deuticke) 1987.

HOINKES, G. & THÖNI, M.: New Findings of Eclogites within the Eoalpine Amphibolite grade Area of the Ötztal Basement. – Terra cognita, **7**, 96, Strasbourg 1987.

HUMPHRIES, F. J. & CLIFF, R. A.: Sm-Nd dating and cooling history of Scourian Granulites, Sutherland. – Nature, **295**, 515–517, London 1982.

HUNZIKER, J. C.: Rb-Sr and K-Ar Age Determination and the Alpine Tectonic History of the Western Alps. – Mem. Ist. Geol. Mineral. Univ. Padova, **31**, 1–54, Padova 1974.

HUNZIKER, J. C., FREY, M., CLAUER, N., DALLMEYER, R. D., FRIEDRICHSEN, H., FLEMING, W., HOCHSTRASSER, K., ROGGWILER, P. & SCHWANDER, H.: The evolution of illite to muscovite: mineralogical and isotopic data from the Garus Alps, Switzerland. – Contrib. Mineral. Petrol., **92**, 157–180, Heidelberg 1986.

HURFORD, A. J.: Cooling and uplift patterns in the Lepontine Alps South Central Switzerland and an age of vertical movement on the Insubric fault line. – Contrib. Mineral. Petrol., **92**, 413–427, Heidelberg 1986.

KIRBY, St. H.: Tectonic Stresses in the Lithosphere: Constraints Provided by the Experimental Deformation of Rocks. – Jour. Geophys. Res., **85**, 6353–6363, Washington 1980.

KLEINSCHRODT, R.: Evolution and kinematic interpretation of Alpine fabrics in the Altkristallin south of the western Tauern window (South Tyrol/Italy). – Terra cognita, **7**, 60, Strasbourg 1987.

KRALIK, M.: Interpretation of K-Ar and Rb-Sr Data from Fine Fractions of Weakly Metamorphosed Shales and Carbonate Rocks at the Base of the Northern Calcareous Alps (Salzburg, Austria). – Tschermaks min. petr. Mitt., **32**, 49–67, Wien 1983.

LAUBSCHER, H. P.: Detachment, shear, and compression in the central Alps. – In: R. D. HATCHER, H. WILLIAMS & I. ZIETZ (Eds.): Contributions to the Tectonics and Geophysics of Mountain Chains, 191–211, Boulder/Col. 1983.

LISTER, G. S. & SNOKE, A. W.: S-C Mylonites. – Jour. Struct. Geol., **6**, 617–638, Oxford 1984.

MADER, P.: Geologie des Lischana-Gebietes, Gemeinde Scuol (Gr.). – Unpubl. Diplom-Arbeit ETH Zürich, 81 S., Zürich 1983.

MASCH, L.: Untersuchung der Aufschmelzung und Deformation der Pseudotachylite der Silvretta (Österreich, Schweiz). – N. Jb. Miner. Mh., **1973**, H. 11, 485–509, Stuttgart 1974.

MASCH, L., WENK, H. R. & PREUSS, R.: Electron microscopy study of hyalomylonites – evidence for frictional melting in landslides. – Tectonophysics, **115**, 131–160, Amsterdam 1985.

MILLER, J. A., HOINKES, G. & THÖNI, M.: ^{40}Ar-^{39}Ar stepheating applied to polymetamorphic terrains – the evolution of the eo-Alpine metamorphism in the western Austroalpine nappes of the Eastern Alps. – Submitted to Tectonophysics 1987.

MORAUF, W.: Die permische Differentiation und die alplidische Metamorphose des Granitgneises von Wolfsberg, Koralpe, SE-Ostalpen, mit Rb-Sr- und K-Ar-Isotopenbestimmungen. – Tschermaks min. petr. Mitt., **27**, 169–185, Wien 1980.

NORRIS, R. J. & HENLEY, R. W.: Dewatering of a metamorphic pile. – Geology, **4**, 333–336, Boulder/Col. 1976.

OBERHÄNSLI, R., HUNZIKER, J. C., MARTINOTTI, G. & STERN, W. B.: Geochemistry, Geochronology and Petrology of Monte Mucrone: An Example of Eo-Alpine Eclogitization of Permian Granitoids in the Sesia-Lanzo Zone, Western Alps, Italy. – Chemical Geology (Isotope Geosci. Sect.), **52**, 165–184, Amsterdam 1985.

OBERHAUSER, R.: Mikrofossilfunde im Nordwestteil des Unterengadiner Fensters sowie im Verspalaflysch des Rätikon. – Jb. Geol. B.-A., **126**/1, 71–93, Wien 1983.

OXBURGH, E. R. & ENGLAND, Ph. C.: Heat flow and the metamorphic evolution of the Eastern Alps. – Eclogae geol. Helv., **73**/2, 379–398, Basel 1980.

PASSCHIER, C. W. & SIMPSON, C.: Porphyroclast systems as kinematic indicators. – Jour. Struct. Geol., **8**/8, 831–843, Oxford 1986.

PFIFFNER, O. A. & RAMSAY, J. G.: Constraints on Geological Strain Rates: Arguments From Finite Strain States of Naturally Deformed Rocks. – Jour. Geophys. Res., **87**/B1, 311–321, Washington 1982.

PHILPOTTS, A. R.: Origin of pseudotachylites. – Am. J. Sci., **262**, 1008–1035, New Haven /Conn. 1964.

PLATT, J. P.: Dynamics of orogenic wedges and the uplift of high-pressure metamorphic rocks. – Geol. Soc. Amer. Bull., **97**, 1037–1053, Boulder/Col. 1986.

PLATT, J. P. & VISSERS, R. L. M.: Extensional structures in anisotropic rocks. – Jour. Struct. Geol., **2**/4, 397–410, Oxford 1980.

PURDY, J. W. & JÄGER, E.: K-Ar Ages on Rock-Forming Minerals from the Central Alps. – Mem. Ist. Geol. Min. Univ. Padova, **30**, 1–31, Padova 1976.

RAMSAY, J. G. & HUBER, M. I.: The Techniques of Modern Structural Geology, volume 2: Folds and Fractures. – 700 pp., London (Academic Press) 1987.

RATSCHBACHER, L.: Kinematics of Austro-Alpine cover nappes: changing translation path due to transpression. – Tectonophysics, **125**, 335–356, Amsterdam 1986.

RUDOLPH, J.: Tieferes Teritär im oberen Fimbertal. – N. Jb. Geol. Paläont. Mh., **1982**, 181–183, Stuttgart 1982.

SATIR, M.: Die Entwicklungsgeschichte der westlichen Hohen Tauern und der suedlichen Oetztalmasse auf Grund radiometrischer Altersbestimmungen. – Mem. Ist. Geol. Min. Univ. Padova, **30**, 1–84, Padova 1975.

SCHMID, S. M. & HAAS, R.: The transition from near surface thrusting to intrabasement décollement along the Schlinig thrust. – Terra cognita, **7**, 68, Strasbourg 1987.

SCHMIDT, K., JÄGER, E., GRÜNENFELDER, M. & GRÖGLER, N.: Rb-Sr und U-Pb-Altersbestimmungen an Proben des Ötztalkristallins und des Schneeberger Zuges. – Eclogae geol. Helv., **60**/2, 529–536, Basel 1967.

SCHMUS, VAN W. R. & BICKFORD, M E.: Rotation of Rb-Sr Isochrons During Low-Grade Events. – ECOG IV, Vol. of Abstracts, p. 95, Amsterdam 1976.

SEGALL, P. & SIMPSON, C.: Nucleation of ductile shear zones on dilatant fractures. – Geology, **14**, 56–59, Boulder/Col. 1986.

SHACKLETON, R. M. & RIES, A. C.: The relation between regionally consistant stretching lineations and plate motions. – J. Struct. Geol., **6**/1–2, 111–117, Oxford 1984.

SHAND, S. J.: The pseudotachylyte of Parijs (Orange Free State). – Geol. Soc. London Quart. Jour., **72**, 198–221, London 1916.

SHI, Y. & WANG, C.-Y.: Two-dimensional modeling of the P-T-t paths of regional metamorphism in simple overthrust terrains. – Geology, **15**, 1048–1051, Boulder/Colorado 1987.

SIBSON, R. H.: Generation of pseudotachylite by ancient seismic faulting. – Geophys. J. R. astr. Soc., **43**, 775–794, Edinburgh – London 1975.

SIMPSON, C.: Borrego Springs – Santa Rosa mylonite zone: A Late Cretaceous west-directed thrust in southern California. – Geology, **12**, 8–11, Boulder/Col. 1984.

SIMPSON, C.: Deformation of granitic rocks across the brittle-ductile transition. – Jour. Struct. Geol., **7**/5, 503–511, Oxford 1985.

SIMPSON, C. & SCHMID, S. M.: An evaluation of criteria to deduce the sense of movement in sheared rocks. – Geol. Soc. Am. Bull., **94**, 1281–1288, Boulder/Col. 1983.

SINHA, A. K., HEWITT, D. A. & RIMSTIDT, J. D.: Fluid interaction and element mobility in the development of ultramylonites. – Geology, **14**, 883–886, Boulder/Col. 1986.

SPRAY, J. G.: Artificial generation of pseudotachylyte using friction welding apparatus: simulation of melting on a fault plane. – Jour. Struct. Geol., **9**/1, 49–60, Oxford 1987.

STEIGER, R. H. & JÄGER, E.: Subcommission on Geochronology: Convention on the use of Decay Constants in Geo- and Cosmochronology. – Earth Plan. Sci. Lett., **36**, 359–362, Amsterdam 1977.

STÖCKHERT, B.: K-Ar determinations on muscovites and phengites from deformed pegmatites, and the minimum age of the Old Alpine deformation in the Austridic basement to the south of the western Tauern Window (Ahrn valley, Southern Tyrol, Eastern Alps). – N. Jb. Mineral. Abh., **150**, 103–120, Stuttgart 1984.

STÖCKHERT, B., JÄGER, E. & VOLL, G.: K-Ar age determinations on phengites from the internal part of the Sesia Zone, Western Alps, Italy. – Contrib. Mineral. Petrol., **92**, 456–470, Heidelberg 1986.

THÖNI, M.: Degree and Evolution of the Alpine Metamorphism in the Austroalpine Unit W of the Hohe Tauern in the light of K/Ar and Rb/Sr Age Determinations on Micas. – Jb. Geol. B.-A., **124**, 111–174, Wien 1981.

THÖNI, M. with contributions by HOINKES, G.: The Thermal Climax of the Early Alpine Metamorphism in the Austroalpine Thrust Sheet. – Mem. Sci. Geol., **36**, 211–238, Padova 1983.

THÖNI, M.: The Rb-Sr Thin Slab Isochron Method – an Unreliable Geochronologic Method for Dating Geologic Events in Polymetamorphic Terrains? – Mem. Sci. Geol., **38**, 283–352, Padova 1986.

THÖNI, M. & HOINKES, G.: The Southern Ötztal Basement: Geochronological and Petrological Consequences of Eoalpine Metamorphic Overprinting. – In: H. W. FLÜGEL & P. FAUPL (Eds.): Geodynamics of the Eastern Alps, 200–213, Wien (Deuticke) 1987.

TOLLMANN, A.: Plattentektonische Fragen in den Ostalpen und der plattentektonische Mechanismus des mediterranen Orogens. – Mitt. österr. geol. Ges., **69** (1976), 291–351, Wien 1978.

TORRICELLI, G.: Geologie der Piz Lad – Piz Ajüz-Gruppe. – Jber. Naturforsch. Ges. Graubünden, **85**, 1–83, Chur (Bischofsberger & Co.) 1956.

VERSCHURE, R. H., ANDRIESEN, P. A. M., BOELRIJK, N. A. I. M., HEBEDA, E. H., MAIJER, C., PRIEM, H. N. A. & VERDURMEN, E. A. T.: On the thermal stability of Rb-Sr and K-Ar biotite systems: Evidence from coexisting Sveconorwegian (ca. 870 Ma) and Caledonian (ca. 400 Ma) biotites in SW Norway. – Contrib. Mineral. Petrol., **74**, 245–251, Heidelberg 1980.

VOGLER, W. S.: Alpine Structures and Metamorphism at the Pillonet Klippe – a Remnant of the Austroalpine Nappe System in the Italian Western Alps. – Geol. Rundschau, **73**/1, 175–206, Stuttgart 1984.

VOLL, G.: Ein Querprofil durch die Schweizer Alpen vom Vierwaldstätter See zur Wurzelzone – Strukturen und ihre Entwicklung durch Deformationsmechanismen wichtiger Minerale. – N. Jb. Geol. Paläont. Abh., **160**/3, 321–335, Stuttgart 1980.

WAGNER, G. A., REIMER, G. M. & JÄGER, E.: Cooling ages derived by apatite fission track, mica Rb-Sr and K-Ar dating: The uplift and cooling history of the Central Alps. – Mem. Ist. Geol. Min. Univ. Padova, **30**, 1–27, Padova 1977.

WALTHER, J. V. & ORVILLE, P. M.: Volatile Production and Transport in Regional Metamorphism. – Contrib. Mineral. Petrol., **79**, 252–257, Heidelberg 1982.

WENK, H. R.: Are pseudotachylites products of fracture or fusion? – Geology, **6**, 507–511, Boulder/Col. 1978.

WILLIAMS, P. F. & COMPAGNONI, R.: Deformation and metamorphism in the Bard area of the Sesia Lanzo Zone, Western Alps, during subduction and uplift. – J. metamorphic Geol., **1**, 117–140, Oxford 1983.

WINKLER, W. & BERNOULLI, D.: Detrital high-pressure/low temperature minerals in a late Turonian Flysch sequence of the Eastern Alps (Western Austria): Implications for early Alpine tectonics. – Geology, **14**, 598–601, Boulder/Col. 1986.

WISE, D. U., DUNN, D. E., ENGELDER, J. T., GEISER, P. A., HATCHER, R. D., KISH, S. A., ODOM, A. L. & SCHAMEL, S.:

Fault-related rocks: Suggestions for terminology. – Geology, **12**, 391–394, Boulder/Col. 1984.

YARDLEY, B. W. D.: Effect of cooling on the water content and mechanical behaviour of metamorphosed rocks. – Geology, **9**, 405–408, Boulder/Col. 1981.

YORK, D.: Least-Squares Fitting of a Straight Line with Correlated errors. – Earth Plan. Sci. Lett., **5**, 320–324, Amsterdam 1969.

ZEITLER, P. K. & WIJBRANS, J. R.: A reassessment appraised: comment on "Hornblende K-Ar ages and the climax of Tertiary metamorphism in the Lepontine Alps (south-central Switzerland): an old problem reassessed" by ALEXANDER DEUTSCH and RUDOLF H. STEIGER. – Earth Plan. Sci. Lett., **76**, 390–392, Amsterdam 1986.

Manuskript bei der Schriftleitung eingelangt am 10. Februar 1988.